

Dear Editor,

Thank you very much for the good news of acceptance. As requested, dataset modifications are now implemented in PANGAEA and the official DOI is assigned. PANGAEA DOI is then updated in the current version of the manuscript.

Best regards

Jacopo Chiggiato

CNR-ISMAR

1 **Dissolved Inorganic Nutrients in the Western Mediterranean Sea (2004-2017)**

2 Malek Belgacem^{1,2}, Jacopo Chiggiato^{1,*}, Mireno Borghini¹, Bruno Pavoni², Gabriella Cerrati³,
3 Francesco Acri¹, Stefano Cozzi⁴, Alberto Ribotti⁵, Marta Álvarez⁶, Siv K. Lauvset⁷, Katrin Schroeder¹

4 ¹ CNR-ISMAR, Arsenale Tesa 104, Castello 2737/F, 30122 Venezia, Italy

5 ² Dipartimento di Scienze Ambientali Informatica e Statistica, Università Ca' Foscari Venezia,
6 Campus Scientifico Mestre, Italy

7 ³ ENEA, Department of Sustainability, S. Teresa, Marine Environmental center, 19032 Pozzuolo di
8 Lerici (SP), Italy

9 ⁴ CNR-ISMAR, Area Science Park – Basovizza, 34149 Trieste, Italy

10 ⁵ CNR-IAS, Loc. Sa Mardini snc, Torregrande, 9170 Oristano, Italy

11 ⁶ Instituto Español de Oceanografía, IEO, A Coruña, Spain

12 ⁷ NORCE Norwegian Research Centre, Bjerknes Centre for Climate Research, 5007 Bergen, Norway

13 *Corresponding author's email: jacopo.chiggiato@ismar.cnr.it

14

15 **Abstract**

16 Long-term time-series are a fundamental prerequisite to understand and detect climate shifts and
17 trends. Understanding the complex interplay of changing ocean variables and the biological
18 implication for marine ecosystems requires extensive data collection for monitoring, hypothesis testing
19 and validation of modelling products. In marginal seas, such as the Mediterranean Sea, there are still
20 monitoring gaps, both in time and in space. To contribute to filling these gaps, an extensive dataset of
21 dissolved inorganic nutrient observations (nitrate, phosphate, Si and silicate) has been collected
22 between 2004 and 2017 in the Western Mediterranean Sea and subjected to rigorous quality control
23 techniques to provide to the scientific community a publicly available, long-term, quality controlled,
24 internally consistent biogeochemical data product. The data product includes 870 stations of dissolved
25 inorganic nutrients, including temperature and salinity, sampled during 24 cruises. Details of the
26 quality control (primary and secondary quality control) applied are reported. The data are available in
27 PANGAEA

28 | (<https://doi.org/10.1594/PANGAEA.904172>, <https://doi.pangaea.de/10.1594/PANGAEA.904172>,

29 Belgacem et al. 2019)

30 **Keywords:** Mediterranean Sea, Dissolved Inorganic Nutrient, biogeochemistry.

31

32 1 Introduction

33 Dissolved inorganic nutrients play a crucial role in marine ecosystem functioning. They serve as
34 regulators of ocean biological productivity, and are trace elements for biogeochemical cycling as well
35 as for natural and anthropogenic sources and transport processes (Bethoux, 1989; Bethoux et al.,
36 1992). They are also non-conservative tracers, since their distribution vary according to both
37 biological (such as primary production and respiration) and physical (such as convection, advection,
38 mixing and diffusion) processes. Very schematically, inorganic nutrients are continuously consumed
39 by phytoplankton (due to primary production) in the sea surface and regenerated in the mesopelagic
40 layer by bacteria and animals (due to respiration). Moreover, the sinking of organic matter and its
41 decomposition increases the nutrient concentrations in the intermediate and deep-water masses over
42 time. To identify the limiting factors for biological production in the oceans, we need to understand
43 the underlying chemical constraints and especially the macro- and micronutrients spatial and temporal
44 variations. Dissolved inorganic nutrients may be used as tracers of water masses like salinity and
45 temperature, to assess mixing processes, and to understand the biogeochemical circumstances of their
46 formation regions. Understanding the complex interplay of changing ocean variables and the
47 biological implication for marine ecosystems is a difficult task and requires not only modelling, but
48 also extensive data collection for monitoring, hypothesis testing and validation. Monitoring gaps still
49 remain in both in time and space, especially for marginal seas such as the Arctic Ocean or the
50 Mediterranean Sea.

Formattato: Tipo di carattere:
(Predefinito) Times New Roman

Formattato: Tipo di carattere:
(Predefinito) Times New Roman

51 The Mediterranean Sea has been identified as a region significantly affected by ongoing climatic
52 changes, like warming and decrease in precipitation (Giorgi, 2006). In addition, it is a region
53 particularly valuable for climate change research because it behaves like a miniature ocean (Bethoux
54 et al., 1999) with a well-defined overturning circulation characterized by spatial and temporal scales
55 much shorter than for the global ocean, with a turnover of only several decades. Being an
56 intercontinental sea, and subjected to more terrestrial nutrient inputs (river runoff, submarine
57 groundwater discharge) and atmospheric deposition, the Mediterranean Sea has a nitrate to phosphate
58 N:P ratio that is anomalously high compared to the “classical” world's oceans Redfield ratio,
59 indicating a general P-limitation regime, which becomes stronger along a west-to-east gradient. The
60 Mediterranean Sea is therefore a potential model to study global patterns that will be experienced in
61 the next decades worldwide, not only regarding ocean circulation, but also the marine biota (Lejeune
62 et al., 2010). Several environmental variables can act as stressors for marine ecosystems, by which
63 climatically driven ecosystem disturbances are generated (Boyd, 2011). These changes affect, among
64 others, the distribution of biogeochemical elements (including inorganic nutrients) and the functioning
65 of the biological pump and CO₂ regulation.

66 Within this context, the aim of this paper is to compile an extensive dataset of dissolved inorganic
67 nutrient observations (nitrate, phosphate, and silicate) collected between 2004 and 2017 in the
68 Western Mediterranean Sea (WMED), to describe the quality control techniques and to provide the
69 scientific community with a publicly available, long-term, quality controlled, and internally consistent
70 biogeochemical data product, contributing to previously published Mediterranean Sea datasets like the
71 MEDAR/Medatlas (time period:1908–1999), (Fichaut et al., 2003) and the Mediterranean Sea –
72 Eutrophication and Ocean Acidification aggregated datasets v2018 (time period: 1911-2017) provided
73 by EMODnet Chemistry (Giorgetti et al., 2018) available at
74 <https://www.seadatanet.org/Products/Aggregated-datasets>.

75 Both original and quality-controlled data are available in PANGAEA:

76 | <https://doi.org/10.1594/PANGAEA.904172><https://doi.pangaea.de/10.1594/PANGAEA.904172>

77 | Coverage: 44°N-35°S; 6°W-14°E

78 | Location Name: Western Mediterranean Sea

79 | Date start: May 2004

80 | Date end: November 2017

81 | **2 Dissolved inorganic nutrient data collection**

82 | **2.1. The CNR dissolved inorganic nutrient data in the WMED**

83 | Long-term time-series, such as the OceanSites global time series (www.oceansites.org), are a
84 | fundamental prerequisite to understand and detect climate shifts and trends. However, biogeochemical
85 | time-series are still limited to the northern Western Mediterranean Sea (MOOSE network, Coppola et
86 | al., 2019). Yet, inorganic nutrients in the Mediterranean Sea has received more attention in recent
87 | years, and various datasets have been compiled to understand its unique characteristics such as the one
88 | build by the PERSEUS project Consortium (“Policy-oriented marine environmental research in the
89 | southern European seas” - EU FP7 project GA #287600), that included 100 cruises collected during
90 | the project’s lifetime, in addition to those from other projects like SESAME, EU FP7 project GA
91 | #GOCE-036949), and data products such as the MEDAR/Medatlas. In addition to that, the data
92 | assembly system EMODnet Chemistry, a leading infrastructure supported by pan-European directorate
93 | General MARE set up (Martin Miguez et al., 2019, Tintoré et al.,2019).

94 | The dataset presented here consists of 24 oceanographic cruises (Fig. 1, Table 1a and Table 1b)
95 | conducted in the WMED on board of research vessels run by the Italian National Research Council
96 | (CNR) and the Science and Technology Organisation Centre for Maritime Research and
97 | Experimentation (NATO-STO CMRE). All cruises were merged into a unified dataset with 870
98 | nutrient stations and ~ 9666 data points over a period of 13 years (2004-2017). The overall spatial
99 | distribution of the stations covers the whole WMED, but the actual distribution strongly varies

100 depending on the specific cruise and most of the data are collected along sections. At all stations,
101 pressure, salinity and temperature were measured with a CTD-rosette system consisting of a CTD SBE
102 911 plus and a General Oceanics rosette with 24 12L Niskin Bottles. Temperature measurements were
103 performed with the SBE-3/F thermometer with a resolution of 10^{-3} °C; conductivity measurements
104 were performed with the SBE-4 sensor with a resolution of $3 \cdot 10^{-4}$ S/m. The probes were calibrated
105 before and after each cruise. During all CNR cruises, redundant sensors were used for both
106 temperature and salinity measurements.

107 Seawater samples for dissolved inorganic nutrient measurements were collected during the CTD up-
108 cast at standard depths (with slight modifications according to the depth at which the deep chlorophyll
109 maximum was detected). The standard depths are usually 5, 25, 50, 75, 100, 200, 300, 400, 500, 750,
110 1000, 1250, 1500, 1750, 2000, 2250, 2500, 2750, 3000 m. No filtration was employed, nutrient
111 samples were immediately stored at -20 °C. Note that sample storage and freezing duration varied
112 greatly from one cruise to another (Table 3 shows cruises where this exceeded 1 year).

113 **2.2. Analytical methods for inorganic nutrients**

114 For all cruises, nutrient determination (nitrate, orthosilicate and orthophosphate) was carried out
115 following standard colorimetric methods of seawater analysis, defined by Grasshoff et al. (1999) and
116 Hansen and Koroleff (1999). For inorganic phosphate, the method is based on the reaction of the ions
117 with an acidified molybdate reagent to yield a phosphomolybdate heteropoly acid, which is then
118 reduced to a blue-colored compound (absorbance measured at 880 nm). Inorganic nitrate is reduced
119 (with cadmium granules) to nitrite that react with an aromatic amine leading to the final formation of
120 the azo dye (measured at 550 nm). Then, the nitrite separately determined must be subtracted from the
121 total amount measured to get the nitrate concentration only. The determination of dissolved silicon is
122 based on the formation of a yellow silicomolybdic acid reduced with ascorbic acid to blue-colored
123 complex (measured at 820 nm).

124 Nutrient analysis was performed in three laboratories. From 2004 to 2013, all cruises nutrients were
125 analysed by ENEA, while for those of 2015 (cruise #23) and 2017 (cruise #24), nutrient
126 concentrations were analysed by CNR-ISMAR. Referring to Table 1S, four different models of
127 autoanalyzer were used. Measurements from the autoanalyzer were reported in $\mu\text{mol L}^{-1}$. Inorganic
128 nutrient concentrations were converted to the standard unit $\mu\text{mol kg}^{-1}$, using sample salinity from CTD
129 and a mean laboratory analytical temperature of 20°C. Data from nutrient analysis were then merged
130 to ancillary CTD bottle data.

131 **2.3. Reference inorganic nutrient data**

132 In addition to the data collected during the above-mentioned cruises, and in order to perform the
133 secondary quality control (described below), we identified five reference cruises (Table 2), based on
134 their spatial and temporal distribution and the reliability of the measurements (see Fig. 2 –Table.3S
135 Fig.1S). Cruises 06MT20110405 and 06MT20011018 are the only two Mediterranean cruises included
136 in the publicly available Global Ocean Data Analysis Project version 2 (GLODAPv2, Olsen et al.
137 2016). These cruises, conducted on board the R/V Meteor, provide a reliable reference because
138 nutrient analysis strictly followed the recommendation of the World Ocean circulation experiment
139 (WOCE) and the GO-SHIP protocols (Hydes et al., 2010; ,Tanhua et al., 2013). Cruises
140 29AH20140426 and 48UR20070528 are to be included in the CARIMED data product (personal
141 communication by M. Álvarez, in preparation but not yet available) and have undergone rigorous
142 quality control following GLODAP routines. Finally, 29AJ20160818 was carried out in the framework
143 of the MedSHIP programme (Schroeder et al., 2015) and its data are available at
144 <https://doi.org/10.1594/PANGAEA.902293> (Tanhua, 2019).

145 **3 Quality Assurance and quality control methods**

146 Combining inorganic nutrient data from different sources, collected by different operators, stored for
147 different amounts of time, and analysed by multiple laboratories, is not a straightforward task. This is
148 widely recognized in the biogeochemical oceanographic community. Since the 1990s, several studies

149 and programmes (e.g. World Ocean Database, World Ocean Atlas, WOCE) have been devoted to
150 facilitate the exchange of oceanographic data and develop quality control procedures to compile
151 databases by the estimation of systematic errors (Gouretski and Jancke, 2000) to increase the inter-
152 comparability, generate consistent data sets and accurately observe the long-term change.

153 An example of a first quality control procedure is the use of reference materials that are available for
154 salinity (IAPSO, salinity standard by OSIL) and temperature (SPRT, Standard Platinum Resistance
155 Thermometer). As for the inorganic carbon, total alkalinity (Dickson et al., 2003) and inorganic
156 nutrients (Aoyama et al., 2016), certified reference materials (CRM) have been recently made
157 applicable for oceanographic cruises. However, since CRM are not always available or used for
158 biogeochemical oceanographic data, Lauvset and Tanhua (2015) developed a secondary quality
159 control tool to identify biases in deep data. The method suggests adjustments that reduce cruise to
160 cruise biases, increase accuracy and allow for the inter-comparison between data from various sources.
161 This approach, based on a crossover and inversion method (Gouretski and Jancke, 2000; Johnson et
162 al., 2001), was used to generate the CARbon IN Atlantic ocean (CARINA, see Hoppema et al., 2009),
163 GLODAPv2.2019 (Olsen et al., 2019) and PACIFICA (Suzuki et al., 2013) data products.

164 **3.1 Primary Quality control**

165 Each individual cruise was first subjected to a primary quality control (1st QC) that included a check of
166 apparent and extreme outliers in CTD salinity, nitrate, phosphate and silicate. Each parameter included
167 a quality control flag, following standard WOCE flags (Table 3). Surface, intermediate and deep layer
168 were evaluated separately because nutrient observations evolve differently in each layer. The
169 coefficient of variation (CV, defined as standard deviation over mean) was computed for each depth
170 layer. Coefficients of variation in the surface (0-250 db) layer were high (nitrate CV=1.16, phosphate
171 CV=1.005, silicate CV=0.75) due to air-sea interaction (Muniz et al., 2001) occurring in this layer
172 rendering it difficult to flag. These influences are of reduced importance in the intermediate (250-1000
173 db) layer (nitrate CV=0.23, phosphate CV=0.31, silicate CV=0.24) and the deep (>1000 db) layer

174 (nitrate CV=0.15, phosphate CV=0.22, silicate CV=0.14), decreasing the total variance. Flags in the
175 upper and intermediate layer were thus set based on outliers within pressure ranges defined according
176 to standard pressures (0-10, 10-30, 30-60, 60-80, 80-160, 160-260, 260-360, 360-460, 460-560,
177 1000 db).

178 Below 1000 db, flagging included an inspection of nitrate to phosphate (N:P) and nitrate to silicate (N:
179 Si) ratios. The Median and Median Absolute Deviation (MAD) was computed by classes of pressure:
180 we considered as outlier any atypical observation and any value that departs from the median by more
181 than three MADs in the different pressure ranges for each cruise.

182 An overview of the nutrient distribution is provided with scatter plots, showing also the flagged
183 measurements (Fig. 3). Each measurement was flagged 2 (“Acceptable/ measured”) or flagged 3
184 (“Questionable”): 4.1% of nitrate data, 3.37% of phosphate data, 3.16% of silicate data, and 0.07% of
185 CTD salinity data were considered outliers and flagged 3. As highlighted by Tanhua et al. (2010), the
186 primary QC can be subjective depending on the expertise of the person flagging the data, thus flagging
187 could bring in some uncertainties.

188 In order to have a first assessment of the precision of each cruise measurements, the standard deviation
189 of observations deeper than 1000 db was calculated along with averages and standard deviations for
190 each cruise and by subregions to have an overview about nutrient content variability in the deep layer
191 and about the observations spatial spread of individual cruises (Table 4). Following the subdivision of
192 Manca et al. (2004), the WMED has been divided into subregions (Fig.2S, Table 2S) according to the
193 general circulation patterns (details in Manca et al.,2004). Table 4 displays the comparison of standard
194 deviation of deep measurements for each cruise and within subregions. The overall standard deviation
195 between cruises in the deep layer varied between 0.51 and 1.41 $\mu\text{mol kg}^{-1}$ for nitrate, between 0.1 and
196 1.64 $\mu\text{mol kg}^{-1}$ for silicate and between 0.025 and 0.078 $\mu\text{mol kg}^{-1}$ for phosphate. Regional standard
197 deviation of nitrate measurements below 1000 db varied between 0.08 $\mu\text{mol kg}^{-1}$ in the Gulf of Lion
198 (DF2) with cruise #9 and 1.6 $\mu\text{mol kg}^{-1}$ in the Balearic Sea (DS2) observations of cruise #14.

199 Phosphate lowest regional standard deviation was $0.01 \mu\text{mol kg}^{-1}$ found in the observations of cruise
200 #9 in Gulf of Lion (DF2), cruise #10 in Balearic Sea (DS2) and Algerian West (DS3), cruise #14 and
201 cruise # 15 in Tyrrhenian South (DT3), cruise #18 in Algero-Provençal (DF1) and Sardinia Channel
202 (DI1) while the highest standard deviation was $0.1 \mu\text{mol kg}^{-1}$ in the observations of cruise #12 in
203 Algerian West (DS3). As for silicate, the lowest standard deviation was $0.02 \mu\text{mol kg}^{-1}$ observed in
204 cruise #9 measurements of Gulf of Lion subregion (DF2) and the highest deep standard deviation was
205 observed in cruise #6 in its all subregions together with cruise #5 measurement in Tyrrhenian North
206 (DT1) with $1.83 \mu\text{mol kg}^{-1}$ standard deviation.

207 Cruises #3, #6 and #9 had the largest spatial extension (see right side of Fig. 9) with a high number of
208 samples over more than seven subregions (Table 4), the geographical variability of the distribution in
209 dissolved inorganic nutrients results thus in the largest standard deviations. Conversely, cruises with
210 smaller spatial coverages have lower standard deviations. Therefore, a relatively small spatial
211 coverage and high standard deviation is considered as indicative of data with low precision (Olsen et
212 al., 2016). This applies to cruises #1, #5, and #16. Despite the small spatial coverage, samples of
213 nitrate and phosphate of cruise #5 have an overall standard deviation of $1.35 \mu\text{mol kg}^{-1}$ and $0.07 \mu\text{mol}$
214 kg^{-1} , respectively, a high standard deviation pointed out also in the regional standard deviation of deep
215 measurements in Tyrrhenian North (DT1) and South (DT3) . Cruise #1, with few stations in
216 Tyrrhenian North (DT1) and South (DT3) subregions and 21 samples below 1000 db, has an overall
217 standard deviation of $1.25 \mu\text{mol kg}^{-1}$ for nitrate, $0.06 \mu\text{mol kg}^{-1}$ for phosphate and $1.64 \mu\text{mol kg}^{-1}$ for
218 silicate. The regional standard deviation was relatively high for nitrate ($0.51\text{-}1.32 \mu\text{mol kg}^{-1}$),
219 phosphate ($0.02\text{-}0.065 \mu\text{mol kg}^{-1}$) and silicate ($0.53\text{-}1.83 \mu\text{mol kg}^{-1}$). A comparison with the deviations
220 from e.g. cruise # 2, carried out in the same year and e.g. cruise #17 (with a similar cruise track),
221 confirms the lower precision of the data of cruise #1. Similar considerations apply to the quality of
222 nitrate samples ($0.87\text{-}1.02 \mu\text{mol kg}^{-1}$) and silicate ($0.87\text{-}0.9 \mu\text{mol kg}^{-1}$) from cruise #16, covering a

223 small area in Tyrrhenian North (DT1) and South (DT3), compared to cruise #17, carried out in the
224 same regions (right side of Fig. 9 and Table 4).

225 Deep silicate measurements of cruise #6 have twice the overall standard deviation of silicate data of
226 cruise #8 from the same year. Adding to that, in the seven subregions, the regional standard deviation
227 of deep silicate observations was the highest, between 1.04-2 $\mu\text{mol kg}^{-1}$ which was relatively high
228 compared to the surrounding cruises that have observations in the same subregions. This is again
229 suggestive of the limited precision. On the other hand, trying to explain the source of relatively high
230 standard deviations in specific cruises is not always straightforward, as they could stem from a variety
231 of sources, sampling, conservation and analysis. The bottom water in the WMED exhibits a high
232 nutrient content below 1000 db (Table 4), due to the longer residence time. Dividing the WMED into
233 subregions, has effectively removed the natural spatial change in nutrients, making the interpretation
234 of the standard deviation a matter of the precision of the measurements only.

235 In Table 4, deep averages by subregions showed that overall nutrient concentration fluctuated around
236 $7.4 \pm 0.9 \mu\text{mol kg}^{-1}$ for nitrate, $0.3 \pm 0.06 \mu\text{mol kg}^{-1}$ for phosphate and $7.7 \pm 0.8 \mu\text{mol kg}^{-1}$ for silicate,
237 similar findings were reported by Manca et al. (2004). Comparing cruise averages in each region
238 enabled the identification of “suspect” cruises. Cruise #24 has the lowest deep average in nitrate in
239 Algero-Provençal (DF1), Tyrrhenian North (DT1) subregions and Sardinia Channel (DII). As for
240 silicate of cruises #24 and #16 was very low compared to the overall regional average in Liguro-
241 Provençal (DF3) and Tyrrhenian South (DT3) subregions. Deep average of phosphate did not show
242 any outlier cruises in all subregions. Different reasons could explain the low precision in the samples,
243 freezing is one. Although it is a valid preservation method (Dore et al., 1996), the error is higher when
244 samples were not analysed immediately (Segura-Noguera et al., 2011), so the storage time could
245 influence.

246 **3.2 Secondary Quality control: the crossover analysis**

247 The method used to perform the secondary QC on the WMED dissolved inorganic nutrient dataset
248 makes use of the quality-controlled reference data, and the crossover analysis toolbox developed by
249 Tanhua (2010a) and Lauvset and Tanhua (2015). The computational approach is based on comparing
250 the cruise data set to a high-quality reference data set to quantify biases, described in detail in Tanhua
251 et al. (2010b). Here, we summarize the technique with emphasis on inorganic nutrients. The first step
252 consisted of selecting reference data, as described in section 2.3. The second step is the crossover
253 analysis that was carried out using a MATLAB Toolbox (available online: [https://cdiac.ess-
255 dive.lbl.gov/ftp/oceans/2nd_QC_Tool_V2/](https://cdiac.ess-
254 dive.lbl.gov/ftp/oceans/2nd_QC_Tool_V2/)) where crossovers are generated as difference between two
256 cruises using the “running cluster” crossover routine. Each cruise is thus compared to the chosen set of
257 reference cruises. For each crossover, samples deeper than 1000 db are selected within a predefined
258 maximum distance set to 2°arc distance, defined as a crossing region, to ensure the quality of the
259 offset with a minimum number of crossovers and to minimize the effect of the spatial change. The
260 reason to select measurements deeper than 1000 db, is to remove the high frequency variability
261 associated to mesoscale features, biological activity and the atmospheric forcing acting in the upper
262 layers, that might induce changes in biogeochemical properties of water masses. On the other hand,
263 also the deep Mediterranean cannot be considered truly “unaffected” by changes, as it is intermittently
264 subjected to ventilation (Schroeder et al., 2016; Testor et al., 2018) and the real variability can be
265 altered in adjusting data. The computational approach takes this into account, since weights are given
266 to the less variant profile in the crossing region, according to the “confidence” in the determined offset
267 of the compared profiles (i.e. the weighted mean offset of a given crossover-pair is weighted to the
268 depth where the offsets of all compared profiles have the smallest variation which indeed is strongly
269 interlinked with the degree of variance of each profile) (for further details see Lauvset and Tanhua,
2015).

270 Before identifying crossovers, each profile was interpolated using the piecewise cubic Hermite method
271 and the distance criteria outlined in Lauvset and Tanhua (2015), their Table 1a, detailed in Key et al.

272 (2004). The crossover is a comparison between each interpolated profile of the cruise being evaluated
273 and the interpolated profile of the reference cruise. The result is a weighted offset (defined as
274 difference cruise/reference) and a standard deviation of the offset. The standard deviation is indicative
275 of the precision; however, it is important to note that this assumption only works because it is a
276 comparison to a reference, and the absolute offset is indicative of accuracy.

277 The third step consists in evaluating and selecting the suggested correction factor that was applied to
278 the whole water column. The correction factor was calculated from the weighted mean offset of all
279 crossovers found between the cruise and the reference data set, involving a somewhat subjective
280 process.

281 For inorganic nutrients, offsets are multiplicative so that a weighted mean offset > 1 means that the
282 measurements of the corresponding cruise are higher than the measurements of the reference cruise in
283 the crossing region and applying the adjustment would decrease the measured values. The magnitude
284 of an increase or a decrease is the difference of the weighted offset from 1. In general, no adjustment
285 smaller than 2% (accuracy limit for nutrient measurements) is applied (detailed description is found in
286 Hoppema et al., 2009; Lauvset and Tanhua, 2015; Olsen et al., 2016; Sabine et al., 2010; Tanhua et al.,
287 2010b).

288 The last step is the computation of the weighted mean (WM) to determine the internal consistency and
289 quantify the overall accuracy of the adjusted product (Hoppema et al., 2009; Sabine et al., 2010;
290 Tanhua et al., 2009), with the difference that our assessment is based on the offsets with respect to a
291 set of reference cruises. This WM reflects the absolute weighted mean offset of the data set compared
292 to the reference data set, hence the smaller the WM the higher the internal consistency. The accuracy
293 was computed from the individual absolute weighted offsets. The WM, which will be discussed in
294 section 4.4., was computed using the individual weighted absolute offset (D) of number of crossovers

295 (L) and the standard deviation (σ): $WM = \frac{\sum_{i=1}^L D(i)/(\sigma(i))^2}{\sum_{i=1}^L 1/(\sigma(i))^2}$

296 **4 Results of the secondary QC and recommendations**

297 The results of the secondary QC revealed the necessary corrections for nitrate, phosphate and silicate.
298 Four cruises were not considered in the crossover analysis: cruises #7 and #11 do not have enough
299 stations > 1000 db (at least 3 to get valid statistics), while cruises #19 and #21 were outside the spatial
300 coverage of the reference cruises. Cruises that were not used for the crossover analysis are made
301 available in the original dataset but were not included in the final data product (see Supplementary
302 material – Part 2 (A2)).

303 Overall, we found a total number of 73 individual crossovers for nitrate, 72 for phosphate and 54 for
304 silicate. An example of the running cluster crossover output is shown in Fig.4. Results of the crossover
305 analysis is an adjustment factor for each cruise and each nutrient, that are shown in Table 5 and Fig. 5-
306 6-7. The adjustment factor was calculated from the weighted mean of absolute offset summarized in
307 Table 6 and Fig. 3S-4S-5S. Table 6 details the improvement of the weighted mean of absolute offset
308 by cruise prior to and after adjustments, the information is also displayed graphically in Fig. 3S-4S-5S.
309 Cruises are in chronological order in all figures and tables.

310 **4.1 Nitrate**

311 The crossover analysis suggests a significant adjustment for nitrate concentrations on 15 cruises,
312 between 0.94 and 0.98 (for adjustments <1) and between 1.02 and 1.34 (for adjustments >1) (Table 5
313 and Fig.5). Offsets suggest that the deep measurements of cruises #1, #3, #4, #5, #6, #8, #12, #13, #15,
314 #16, #23 and #24 need to be adjusted towards higher concentrations, when compared to the respective
315 reference (Fig.3S).

316 Nitrate observations of cruises #2, #9 and #10 on the other hand were higher than the reference cruises
317 and exhibit variation outside the accepted accuracy limit, thus require a downward adjustment.

318 Finally, five cruises (#14, #17, #18, #20, and #22) were consistent with the reference data and no
319 adjustment was necessary. Considering the weighted mean of absolute offset after adjustments shown
320 in Table 6, two cruises (#5 and #24) required large correction factors but remain outside the accuracy
321 threshold (Fig. 5). These cruises are considered in detail later (section 4.4).

322 **4.2 Phosphate**

323 For phosphate the crossover analysis suggests adjustments for 20 cruises, as shown in Fig. 6. Deep
324 phosphate measurements of 15 cruises (Table 6) appear to be lower than the respective reference
325 measurements (i.e. phosphate data of these cruises require an upward adjustment), while the data of
326 five cruises (#2, #3, #4, #6, #24) are higher (i.e. they need a downward adjustment) (Fig.4S). Applying
327 all the indicated adjustments, the large offsets of cruises #2, #3, #4, #6, #8, #9, #10, #18, #20, #23 and
328 #24 are reduced and became consistent with the reference. Cruises #1, #5, #12, #13, #14, #15, #16,
329 #17, and #22 retain an offset even after applying the indicated adjustment. These cruises are
330 considered in detail later.

331 According to Olsen et al. (2016), if a temporal trend is detected in the offsets, no adjustments should
332 be applied. There is indeed a decreasing trend between 2008 and 2017 in the phosphate correction
333 factor (Fig. 6), and thus an increasing one in the weighted mean offset (Fig.4S), implying a temporal
334 increase of phosphate. Therefore, phosphate data of the cruises being part of the trend were not
335 flagged as questionable, except some cruises that are discussed further in section 4.4.

336 Comparing phosphate before and after adjustment, the corrections did minimise the difference with the
337 reference, while the actual variation with time was preserved (Fig.6). The temporal trend towards
338 higher phosphate concentrations in the Mediterranean Sea is considered to be real, even though
339 studies concerning the biogeochemical trends in the deep layers of the WMED are scarce (Pasqueron
340 et al., 2015). However, this variation could be consistent with the findings of Béthoux et al.(1998,
341 2002) and the modelling studies by Moon et al. (2016) and Powley et al. (2018) who indeed found an

342 increasing trend in phosphate concentrations over time, due to the increase in the atmospheric and
343 terrestrial inputs.

344 **4.3 Silicate**

345 The results of the crossover analysis for silicate suggests corrections for all cruises (Fig.7). The
346 crossovers indicate that deep silicate measurements are lower in the evaluated cruises than in the
347 corresponding reference cruises (i.e. they need to be adjusted upward) (Fig.5S). This is likely to be a
348 direct result of freezing the samples before analysis, since the reactive silica polymerizes when frozen
349 (Becker et al., 2019). After applying the adjustment (Table 5), as expected, the offsets are reduced
350 (Table 6), but five cruises (#1, #5, #6, #15, and #16) remain outside the accuracy envelope. Due to the
351 large offsets, these cruises will be discussed further in section 4.4.

352 **4.4 Discussion and recommendation**

353 Adjustments were evaluated for each cruise separately. As a general rule, no correction was applied
354 when the suggested adjustment is strictly within the 2% limit (indicated with NA in Table 5). The
355 average correction factors were 1.06 for nitrate, 1.14 for phosphate and 1.14 for silicate, respectively.
356 To verify the results, we re-ran the crossover analysis and re-computed offsets and adjustment factors
357 using the adjusted data (as shown in blue in Fig. 3S-4S-5S and Fig. 5-6-7). Most of the new
358 adjustments are within the accuracy envelope and few are outside the limit, except for the cruises
359 belonging to the above mentioned “phosphate-trend” and the other outlying cruises which are detailed
360 hereafter. By the application of adjustments, the deep-water offsets were reduced. This can be seen in
361 the decrease of the weighted mean offset between the data before adjustments (after 1st QC, Fig. 3S-
362 4S-5S, in grey) and the adjusted data (after 2nd QC, Fig. 3S-4S-5S, in blue).

363 Referring to the analysis detailed in section 3.2, the internal consistency of the nutrient data set has
364 improved and increased significantly after the adjustment, from 4% for nitrate, 19% for phosphate and
365 13% for silicate, to a more unified dataset with 3 % for nitrate, 6 % for phosphate and 3% for silicate.

366 A comparison between the original and the adjusted nutrient observations is shown in Fig. 8A-B-C,
367 indicating an improvement in the accuracy based on the reference data and a relatively reduced range
368 particularly for phosphate (Fig. 8B). Figure 8. D-E scatterplots show that after the quality control,
369 nutrient stoichiometry slopes obtained from regressions, between tracers along the water column
370 demonstrate a strong coupling and provide a nitrate to phosphate ratio of ~22.09 and a nitrate to
371 silicate ratio of ~0.94. These values are consistent with nutrient ratios range found in the WMED as
372 reported in Lazzari et al. (2016); Pujo-Pay et al., (2011) and Segura-Noguera et al. (2016). The
373 regression model is more accurate after adjustments with an improved r^2 for N:P (from 0.81 to 0.90)
374 and for N: Si (from 0.85 to 0.87).

375

376 In the following some details on the adjustment of specific cruises are given:

377 Cruise #2 [48UR20041006] needed an adjustment of 0.98 for nitrate, 0.9 for phosphate and 1.06 for
378 silicate. Most of the crossover profiles occur in the Tyrrhenian Sea (Tyrrhenian North and Tyrrhenian
379 South subregions). After adjustment, the cruise is inside the 2% envelope.

380 Cruise #3 [48UR20050412] appeared to be outside the 2% envelope before adjustments. Its offsets
381 with five reference cruises, crossing the Tyrrhenian Sea, Sardinia Channel, Gulf of Lion and Algero-
382 Provençal subregions, showed that nitrate and silicate values to be relatively low, and thus an
383 adjustment of 1.08 and 1.15 was applied respectively. On the other hand, phosphate values were
384 relatively high, and a 0.93 adjustment was applied.

385 Cruise #4 [48UR20050529] correction factor estimate was based on five crossovers that covered five
386 subregions: Tyrrhenian South, Sardinian Channel, Algerian East and West and the Alboran Sea. Table
387 4 show that there are no large differences between regional averages within the cruise which justify an
388 adjustment of 1.04 for nitrate, 0.85 for phosphate and 1.183 for silicate.

389 Cruise #8 [48UR20060928] was adjusted by 1.03 for nitrate, 1.14 for phosphate and 1.1 for silicate,
390 because it showed values to be low compared to four references. After adjustment, the data were
391 inside the acceptable range.

392 Cruise #9 [48UR20071005] values of nitrate were slightly outside the 2% envelope before
393 adjustments, similar to phosphate and silicate that were lower compared to the reference. The
394 adjustments of 0.97 for nitrate, 1.14 for phosphate and 1.115 for silicate suggested by the mean offset
395 against the reference cruises were recommended.

396 Cruise #13 [48UR20090508] has three crossovers in the common crossing zone that included
397 Tyrrhenian North, Tyrrhenian South and Sardinia Channel subregions. The crossover suggests that this
398 cruise has too low values and needs an adjustment of 1.05 for nitrate, 1.33 for phosphate and 1.15 for
399 silicate.

400 Cruise #14 [48UR20100430] has a mean offset with four reference cruises that suggests an adjustment
401 factor of 1.34 for phosphate and 1.123 for silicate. Nitrate did fall within the accuracy envelope; no
402 adjustment was needed.

403 Cruise #10 [48UR20080318] has only three crossovers in the Algero-Provençal subregion, showing
404 that nitrate is too high compared to the reference while phosphate and silicate are slightly lower. We
405 therefore applied the adjustments of Table 5, since the deep averages in each region (Table 4) did not
406 show large regional difference.

407 Cruise #17 [48UR20110421] crossover analysis did not suggest any correction for nitrate; however,
408 with an offset based on two crossovers in the Tyrrhenian North and South subregions, adjustments
409 were recommended for phosphate (1.25) and silicate (1.12), for being lower than the reference cruises.

410 Cruise #18 [48UR20111109] is similar to cruise #17, since it was suggested to adjust phosphate by
411 1.14 and silicate by 1.09, based on four crossovers in the Tyrrhenian North and South, Sardinia
412 Channel and Algero-Provençal subregions.

413 Cruise #20 [48UR20120111] has four crossovers over the Tyrrhenian North and South and Algero-
414 Provençal subregions. Its measurements were slightly lower than the reference cruises suggesting a
415 correction factor of 1.17 for phosphate and 1.08 for silicate.

416 Cruise #22 [48UR20131015] has similar correction factors as cruise #20, based on three crossovers in
417 the Sardinia Channel and Tyrrhenian North and South subregion, with measurements being lower than
418 the reference.

419 Cruise #23 [48QL20150804] showed nutrient values slightly lower than the reference cruises as well,
420 suggesting small correction factors of 1.02 for both nitrate and phosphate and 1.08 for silicate, a
421 correction factors that were based on offsets with five cruises.

422 Below, we discuss the recommended flags in the final product (Table 3; see supplementary Materials
423 Part-2 (A2)) assigned for some cruises that needed further consideration, since they required larger
424 adjustment factors:

425 Cruise #1 [48UR20040526]: The adjusted values are still lower than the reference (Fig.5-6-7-Fig.3S-
426 4S-5S) and are still outside the 2% accuracy range. This cruise had stations in the Sicily Strait,
427 Tyrrhenian North and South and Ligurian East subregions (Fig. 9, right side) and only 4 stations were
428 deeper than 1000 db (those within the Tyrrhenian Sea). The low precision of this cruise has already
429 been evidenced during the 1st QC (section 3.1). We recommend flagging this cruise as questionable
430 (flag 3).

431 Cruise #5 [48UR20051116]: This cruise took place between Sicily Strait and the Tyrrhenian North and
432 South (Fig. 9, right side). Nitrate, phosphate and silicate data were lower than those from other cruises

433 (#3 and #4) run the same year (Fig. 5-6-7-Fig.3S-4S-5S) and are still biased after adjustments.
434 Considering the limited precision and the low number of crossovers, it is recommended to flag the
435 cruise as questionable (flag 3).

436 Cruise #6 [48UR20060608]: This cruise had an offset with five cruises giving evidence that
437 adjustments of 1.05 for nitrate, 0.86 for phosphate and 1.26 for silicate are needed. The silicate bias
438 was reduced after adjustment but remained large with respect to the accuracy limit (Fig. 7-Fig. 5S).
439 This cruise has a wide geographic coverage, with stations along 9 sections (Fig. 9, right side).
440 Considering also the high standard deviation (Table 4), which is partially attributed to the spatial
441 coverage of the cruise, there is still uncertainty about the quality of the samples. It is recommended to
442 flag silicate data of cruise #6 as questionable (flag 3).

443 Cruise #12 [48UR20081103]: Phosphate data have low accuracy with respect to the reference cruises
444 (Fig. 6-Fig. 4S). This cruise has stations along a longitudinal section from Sicily Strait to the Alboran
445 Sea, which might explain the large standard deviation of deep phosphate samples (Table 4). Cruise
446 #12 was given a correction of 1.08 for nitrate, 1.12 for silicate and 1.38 for phosphate. The mean
447 offset from five crossovers computed within the Tyrrhenian South, Sardinia Channel, Algerian East,
448 Algerian West and Alboran Sea subregions suggests that this cruise has lower nutrient values than the
449 reference cruise. After adjustment, cruise #12 is within the acceptable range for nitrate and silicate but
450 not for phosphate as highlighted in section 3.2. In addition, considering the relatively high number of
451 stations >1000 db and a plausible trend in phosphate, it is recommended to flag the phosphate data as
452 good/acceptable (flag 2).

453 Cruise #15 [48UR20100731]: This cruise has 149 station along a similar track as cruise #12 but shows
454 larger offsets for phosphate and silicate (Fig. 6-7-Fig. 4S-5S), compared to cruise #12. Considering
455 that deep silicate data was not of low quality (small standard deviation, see Table 4), and that deep
456 phosphate fall within the “phosphate-trend” discussed above, these data are flagged good/acceptable
457 (flag 2).

458 Cruise #16 [48UR20101123]: The cruise shows large offsets for phosphate and silicate (Fig. 6-7- Fig.
459 4S-5S), similar to cruise #15. Considering that the overall cruise standard deviation of silicate samples
460 below 1000 db was relatively high (1.02 over 14 samples, see Table 4), and that it has only one
461 crossover between the Tyrrhenian North and South subregions (Table 6), and that when comparing
462 deep regional averages, this cruise had the lowest average silicate value, it is recommended to flag
463 silicate data of cruise #16 as questionable (flag 3). As for phosphate, the cruise is part of the
464 “phosphate-trend” and is therefore flagged good/acceptable (flag 2).

465 Cruise #24 [48QL20171023]: This cruise has the largest offset for nitrate even after adjustment. It is
466 very likely due to a difference between laboratories (calibration standards) concerning nitrate, which
467 needs to be flagged as questionable (flag 3) in the final product.

468 There are several sources of bias in the observation. One of the main reasons for an upward/
469 downward bias would be the difference in the nutrient’s chemical analytical method and the lack of
470 use of CRM in all cruises as also noted in CARINA (Tanhua et al., 2009) or in the most recent global
471 comparability study by Aoyama (2020).

472 Cruises discussed in this section were not removed from the final product but are retained along with
473 their recommended quality flag (Table 3) detailed above and in the supplementary material – Part 2
474 (A2)). We have done the evaluation of their overall quality but leave it up to the users how to
475 appropriately use these data.

476 **4.5 Product assessment: Comparison with MEDATLAS**

477 Averages water mass biogeochemical properties have been computed from the adjusted product (Table
478 7), and compared to the MEDAR/Medatlas annual climatological profiles, downloaded from the
479 Italian NODC website (<http://doga.ogs.trieste.it/medar/>) given by Manca et al. (2004), in order to
480 evaluate and asses the new product. Since nutrient properties exhibit differences with depths, we

481 compared average nutrient concentrations of the three main water masses in twelve subregions of the
482 WMED (Table 7, Fig 2S).

483 The results of Table 7 compares water mass biogeochemical properties with the reference climatology.
484 The new product agrees well with the Medatlas climatology. However, there are some distinctions.
485 The surface layer (0-150db) is characterized by a low nutrient content. The surface nitrate varies
486 between 0.69 and 2.75 $\mu\text{mol kg}^{-1}$ with a maximum found in the Ligurian East (DF4) and the minimum
487 in the Alboran Sea (DS1) subregions, similar values were recorded in the climatology (0.61- 3.00
488 $\mu\text{mol kg}^{-1}$). The differences in nitrate averages in the surface layer are observed in the Gulf of Lion
489 (DF2) where the new product is higher than the climatology and slightly lower in the Liguro-
490 Provençal (DF3). As for, the surface content in phosphate, it varied between 0.04 and 0.16 $\mu\text{mol kg}^{-1}$
491 with a maximum found in the Ligurian East (DF1) and a minimum in the Alboran Sea (DS1), alike the
492 Medatlas climatology, where phosphate averages fluctuate between 0.05 and 0.19 $\mu\text{mol kg}^{-1}$. The new
493 product is slightly lower compared to the climatology. As to the average surface in silicate, it varies
494 between 1.36 and 2.91 $\mu\text{mol kg}^{-1}$ with a minimum found in the Ligurian East (DF4), the maximum in
495 the Gulf of Lion (DF2)) while in the climatology, it varied between 1.27 and 2.31 $\mu\text{mol kg}^{-1}$ (the
496 minimum in the Ligurian East (DF4) and the maximum in the Alboran Sea (DS1)). The new product is
497 slightly higher in silicate.

498 Overall, the differences in the surface layer are observed in the Gulf of Lion (DF2), the Liguro-
499 Provençal (DF3) and the Ligurian East (DF4) regions which could be due to the intense variability of
500 the vertical mixing occurring in the northern WMED compared to the other subregions.

501 In the intermediate layer, averages were computed from the depth of the salinity maximum (S_{max})
502 $\pm 100\text{m}$ from a regional average profile, indicative of the Levantine Intermediate Water (LIW) core.
503 Nitrate average varied between 4.94 and 9.32 $\mu\text{mol kg}^{-1}$ where the minimum content was recorded in
504 Sicily strait (DI3) and the maximum in the Algerian West (DS3) while in the Medatlas climatology,
505 nitrate was between 5.14 and 8.60 $\mu\text{mol kg}^{-1}$. In average, the lowest content in nitrate was in the

506 Tyrrhenian North (DT1) and South (DT3), Sardinia Channel (DI1) and Sicily Strait (DI3) while LIW
507 of the Gulf of Lion (DF2), Liguro-Provençal (DF3), Ligurian East (DF4), Balearic Sea (DS2), Algero-
508 Provençal (DF1), Alboran Sea (DS1), Algerian West (DS3) and East (DS4) subregions was relatively
509 rich in nitrate. Compared to the Medatlas product, though the new product was slightly higher mainly
510 in the Gulf of Lion (DF2), Ligurian East (DF4) and Balearic Sea (DS2). As for phosphate, LIW
511 averages showed similar behavior as nitrate, the lowest phosphate content ($0.21-0.27 \mu\text{mol kg}^{-1}$) was
512 observed in the Eastern subregions of WMED (DI3,DI1, DT3 and DT1), when the maximum
513 concentrations ($0.4-0.37 \mu\text{mol kg}^{-1}$) were reported in the Western subregions of the WMED (DS1, DS3
514 and DS4, DS2 and DF2). The large differences between the two products were in the Ligurian East
515 (DF4) and the Alboran Sea (DS1), subregions of few numbers of observations.

516 Concerning silicate, the lowest average concentration ($5.25 \mu\text{mol kg}^{-1}$) was observed in LIW core of
517 Sicily Strait (DI3,) and the maximum concentrations ($8.66 - 8.77 \mu\text{mol kg}^{-1}$) were in the Alboran Sea
518 (DS1) and Gulf of Lion (DF2), similar values were recorded in the Medatlas climatology ($4.86-7.95$
519 $\mu\text{mol kg}^{-1}$). There are some discrepancies, where the new product was higher particularly in the Gulf
520 of Lion (DF2), Liguro-Provençal (DF3) and Algerian West (DS3) subregions. This difference is
521 explained by the limited number of observations within depth range in the new product compared to
522 the observations used in the climatology in these subregions.

523 Referring to Manca et al.,(2004), the LIW core salinity values are relatively more pronounced in Sicily
524 Strait (DI3), Sardinia Channel (DI1) and in the Tyrrhenian South (DT3) and North (DT1) subregions,
525 where nutrients were lower than the Western subregions (DS3, DS4, DS1 , DF1, DS2, DF4, DF3,
526 DF2). The averages of nutrient within the LIW core ties well with the Medatlas climatology averages
527 (Table 7), except in subregions with important vertical mixing.

528 We have verified also average biochemical properties in the deep layer (below 1500db). The new
529 product is slightly higher in nitrate averages ($7.74 -8.37 \mu\text{mol kg}^{-1}$) than the Medatlas climatology
530 ($7.12 - 8.06 \mu\text{mol kg}^{-1}$) (Table 7). The largest difference was found in Tyrrhenian South (DT3) and

531 North (DT1) subregions. This difference could be due to the fact that, we are comparing two different
532 time periods (2004-2017 and 1908-2001). As for the deep layer phosphate, average concentrations
533 varied between 0.35 and 0.37 $\mu\text{mol kg}^{-1}$ and were within the climatology limits (0.31 - 0.40 $\mu\text{mol kg}^{-1}$).
534 In all subregions, there was not large differences. Overall, phosphate was in accordance with the
535 Medatlas climatology. Similar to nitrate, deep average silicate in the new product (8.64 -9.21 $\mu\text{mol kg}^{-1}$)
536 was higher than the climatology (7.51 to 9.04 $\mu\text{mol kg}^{-1}$). The largest difference in average silicate
537 was observed in the Tyrrhenian North (DT1), South (DT3) and Liguro-Provençal (DF3) subregions.

538 We then used the Root Mean Squared Error (RMSE) as statistical index to quantify the difference
539 between averaged regional profiles from the new product and Medatlas product. The climatology
540 annual profiles were interpolated to the regional average profiles of the new product, and the average
541 RMSE for each layer and subregion was calculated. Fig. 10 shows the regional evolution of RMSE in
542 the main water masses for the three nutrients. For nitrate (Fig. 10 A), the RMSE in the surface layer
543 varied between 0.12 $\mu\text{mol kg}^{-1}$ (in the Tyrrhenian North (DT1)) and 1.36 $\mu\text{mol kg}^{-1}$ (in the Gulf of
544 Lion (DF2)); in the intermediate layer, the RMSE was between 0.07 $\mu\text{mol kg}^{-1}$ (in the Sardinia
545 Channel (DI1)) and 2.35 $\mu\text{mol kg}^{-1}$ (in the Gulf of Lion (DF2)), and was lower in the deep layer,
546 between 0.11 $\mu\text{mol kg}^{-1}$ (in the Algerian East (DS4)) and 0.79 $\mu\text{mol kg}^{-1}$ (the Gulf of Lion (DF2)). The
547 RMSE decreases in the Algerian East (DS4), Tyrrhenian North (DT1), Tyrrhenian South (DT3),
548 Sardinia Channel (DI1) and Sicily Strait (DI3). This illustrates the low difference between the two
549 products.

550 For phosphate (Fig. 10 B), the RMSE ranges between 0.0022 $\mu\text{mol kg}^{-1}$ (in the Tyrrhenian South
551 (DT3)) and 0.12 $\mu\text{mol kg}^{-1}$ (in the Ligurian East (DF4)) in the surface layer; and is between 0.003
552 $\mu\text{mol kg}^{-1}$ (in the Liguro-Provençal subregion (DF3)) and 0.048 $\mu\text{mol kg}^{-1}$ (in the Alboran Sea (DS1))
553 at intermediate depths, while in the deep layer RMSE varied between 0.0087 (in the Gulf of Lion
554 (DF2)) and 0.057 $\mu\text{mol kg}^{-1}$ (in the Tyrrhenian North (DT1)).

555 Regarding silicate RMSE (Fig. 10 C) in surface, it varied between $0.13 \mu\text{mol kg}^{-1}$ (in the Algero-
556 Provençal subregion (DF1)) and $3.5 \mu\text{mol kg}^{-1}$ (in the Ligurian East subregion (DF4)), A lower RMSE
557 between $0.10 \mu\text{mol kg}^{-1}$ (in the Sardinia Channel (DI1)) and $2.54 \mu\text{mol kg}^{-1}$ (in the Gulf of Lion (DF2))
558 was reported in the intermediate layer; the results in deep layer, were between $0.33 \mu\text{mol kg}^{-1}$ (in the
559 Algerian East (DS4)) and $1.43 \mu\text{mol kg}^{-1}$ (in the Liguro-Provençal subregion (DF3)).

560 The best agreement between the two products was observed in the intermediate and deep layer. The
561 lowest RMSE was confined to the deep layer in most of the subregions while the highest difference
562 was found in the surface layer since it is subjected to intense vertical mixing mainly in the northern
563 WMED. Comparing averages in subregions, showed similar differences in nutrient between the two
564 products particularly in the Gulf of Lion (DF2), the Liguro-Provençal (DF3), Ligurian East (DF4) and
565 Algerian East (DS4), due to the relative high variability in nutrient concentrations in these subregions.
566 These differences are not significant as there is discrepancy on the number of observations used in the
567 two products. Overall, inorganic nutrients of the new product agree very well with the
568 MEDAR/Medatlas climatology. The main features of the spatial distribution in the inorganic nutrients
569 were in accordance with the findings of Manca et al., (2004), where the relative high content in
570 nutrient was found in the intermediate layer of the Algerian subregions (DF1, DS3, DS4) than in other
571 subregions (Table 7). Besides, the highest concentrations in deep layer silicate were reported in the
572 Algerian subregions in the two products ($9.21 \mu\text{mol kg}^{-1}$ (DS3) in the new product; $9.04 \mu\text{mol kg}^{-1}$
573 (DS4) in the climatology), which is indicative of the poor regional ventilation and of the longer
574 residence time of deep water especially in these subregions.

575 **5 Final remarks**

576 An internally consistent data set of dissolved inorganic nutrients has been generated for the WMED
577 (2004-2017). The accuracy envelope for nitrate and silicate was set to 2%, a predefined limit used in
578 GLODAP and CARINA data products. Regarding phosphate data, these were almost entirely outside
579 this limit, because of its natural variations and the overall very low concentrations in the WMED, a

580 highly P-limited basin. Using a crossover analysis (2nd QC toolbox) to compare cruises with respect to
581 reliable reference data, improved the accuracy of the measurements by bias-minimizing the individual
582 cruises. The new product was broadly in consistent with the earlier climatology MEDAR/Medatlas.

583 The publication of a quality-controlled extensive (spatially and temporally) database of inorganic
584 nutrients in the WMED was timely and fills a gap in information that prevented baseline assessments
585 on spatial and temporal variability of biogeochemical tracers in the Mediterranean. In combination
586 with older databases in the same region (e.g. bottle data available in the MEDAR/Medatlas database),
587 this new data producte will thus constitute a pillar on which the Mediterranean marine scientific
588 community will be able to build on original research topics on biogeochemical fluxes and cycles and
589 their relation to hydrological changes that occurred in the period covered by the dataset. The dataset is
590 also relevant for the modelling community as it can be used as an independent data product to assess
591 reanalysis products or it can be assimilated in new reanalysis products.

592 **6 Data availability**

593 The final product is available as a .csv merged file from PANGAEA, and can be accessed at
594 <https://doi.org/10.1594/PANGAEA.904172><https://doi.pangaea.de/10.1594/PANGAEA.904172>
595 (Belgacem et al. 2019).

596 Ancillary information is in the supplementary materials with the list of variables included in the
597 original and final product. Table 1a and Table 1b summarizes all cruises included in the dataset. The
598 dataset include frequently measured stations and key transects of the WMED with in situ physical and
599 chemical oceanographic observations. As mentioned, two files are accessible, both include
600 oceanographic variables observed at the standard depths (see supplementary Materials Part-2).

601 - *Original dataset: CNR_DIN_WMED_20042017_original.csv*: This is the original dataset with
602 flag variable for each of the following parameter: CTD salinity, nitrate, phosphate and silicate
603 from the primary quality control (detailed in section 3.1).

604 - *Adjusted dataset: CNR_DIN_WMED_20042017_adjusted.csv*: This is the product after
605 primary quality control and after applying the adjustment factors from the secondary quality
606 control. Recommendations of section 4.4 are included, as well as quality flags.

607 **Author contribution:** MB, MA, SL, JC and KS substantially contributed to write the manuscript. SC,
608 GC and FA run the chemical analysis and contributed to the manuscript. MB coordinated the technical
609 aspects of most of the cruises. SC, GC, FA, AR, BP contributed in specific part of the manuscript.

610 **Acknowledgements.** The data have been collected in the framework of several of national and
611 European projects, e.g.: KM3NeT, EU GA #011937; SESAME, EU GA #GOCE-036949; PERSEUS,
612 EU GA #287600; OCEAN-CERTAIN, EU GA #603773; COMMON SENSE, EU GA #228344;
613 EUROFLEETS, EU GA #228344; EUROFLEETS2, EU GA # 312762; JERICO, EU GA #262584;
614 the Italian PRIN 2007 program “Tyrrhenian Seamounts ecosystems”, and the Italian RITMARE
615 Flagship Project, both funded by the Italian Ministry of University and Research. We thank Sarah
616 Jutterström from the Swedish Environmental Research institute for the invaluable help in Quality
617 Control discussions. We would like to express our appreciation to the INOCEN laboratory team at
618 IEO for their help and collaboration during MB’s stay there. The authors are deeply indebted to all
619 investigators and analysts who contributed to data collection at sea during so many years, as well as to
620 the PIs of the cruises (S. Aliani, M. Astraldi, M. Azzaro, M. Dibitto, G. P. Gasparini, A. Griffa, J.
621 Haun, L. Jullion, G. La Spada, E. Manini, A. Perilli, C. Santinelli, S. Sparnocchia), the captains and
622 the crews for allowing the collection of this enormous dataset; without them, this work would not have
623 been possible.

624

625

626

627

628

629

630

631

632

633

634

635

636

637

638

639

640

641 **References** Aoyama, M., Woodward, E., Malcolm, S., Bakker, K., Becker, S., Björkman, K., Daniel,
642 A., Mahaffey, C., Murata, A., Naik, H., Tanhua, T., Rho, T., Roman, R. and Sloyan, B.: Comparability
643 of oceanic nutrient data, Poster Cluster Community Whitepaper, CLIVAR Open Science Conference
644 on "Charting the course for climate and ocean research", 18-25 September 2016, Qingdao (China), 12
645 pp., <http://hdl.handle.net/10261/17137>, 2016.

646 Aoyama, M.: Global certified-reference-material-or reference-material-scaled nutrient gridded dataset
647 GND13. Earth System Science Data, 12, 487-499, <https://doi.org/10.5194/essd-12-487-2020>, 2020.

648 Becker, S., Aoyama, M., Woodward, E.M.S., Bakker, K., Coverly, S., Mahaffey, C., and Tanhua, T.:
649 GO-SHIP Repeat Hydrography Nutrient Manual: The precise and accurate determination of dissolved

650 inorganic nutrients in seawater, using Continuous Flow Analysis methods, In: The GO-SHIP Repeat
651 Hydrography Manual: A Collection of Expert Reports and Guidelines, 56 ,
652 <http://dx.doi.org/10.25607/OBP-555>, 2019.

653

654 Belgacem, M., Chiggiato, J., Borghini, M., Pavoni, B., Cerrati, G., Acri, F; Cozzi, S., Ribotti, A.,
655 Álvarez, M., Lauvset, S. K., Schroeder, K.: Quality controlled dataset of dissolved inorganic nutrients
656 in the western Mediterranean Sea (2004-2017) from R/V oceanographic cruises. PANGAEA,
657 <https://doi.org/10.1594/PANGAEA.904172><https://doi.pangaea.de/10.1594/PANGAEA.904172>, 2019.

658 Bethoux, J. P.: Oxygen consumption, new production, vertical advection and environmental evolution
659 in the Mediterranean Sea, Deep Sea Research, Part A, Oceanographic Research Papers, 36(5), 769–
660 781, doi:10.1016/0198-0149(89)90150-7, 1989.

661 Bethoux, J. P., Morin, P., Madec, C. and Gentili, B.: Phosphorus and nitrogen behaviour in the
662 Mediterranean Sea, Deep Sea Research, Part A, Oceanographic Research Paper, 39(9), 1641–1654,
663 doi:10.1016/0198-0149(92)90053-V, 1992.

664 Bethoux, J. P., Gentili, B., Morin, P., Nicolas, E., Pierre, C. and Ruiz-Pino, D.: The Mediterranean
665 Sea : a miniature ocean for climatic and environmental studies and a key for the climatic functioning of
666 the North Atlantic, Progress in Oceanography, 44, 131–146, 1999.

667 Béthoux, J. P., Morin, P., Chaumery, C., Connan, O., Gentili, B. and Ruiz-Pino, D.: Nutrients in the
668 Mediterranean Sea, mass balance and statistical analysis of concentrations with respect to
669 environmental change, Marine Chemistry , 63(1–2), 155–169, doi:10.1016/S0304-4203(98)00059-0,
670 1998.

671 Béthoux, J. P., Morin, P. and Ruiz-Pino, D. P.: Temporal trends in nutrient ratios: Chemical evidence
672 of Mediterranean ecosystem changes driven by human activity, Deep Sea Research Part II Topical
673 Studies in Oceanography, 49(11), 2007–2016, doi:10.1016/S0967-0645(02)00024-3, 2002.

674 Boyd, P. W.: Beyond ocean acidification, Nature Geoscience, 4(5), 273–274, doi:10.1038/ngeo1150,
675 2011.

676 Coppola, L., Raimbault, P., Mortier, L., and Testor, P.: Monitoring the environment in the
677 northwestern Mediterranean Sea, Eos, 100, <https://doi.org/10.1029/2019EO125951>, 2019.

678 Dickson, A. G., Afghan, J. D. and Anderson, G. C.: Reference materials for oceanic CO₂ analysis: A
679 method for the certification of total alkalinity, Marine Chemistry, 80(2–3), 185–197,
680 doi:10.1016/S0304-4203(02)00133-0, 2003.

681 Dore, J. E., Houlihan, T., Hebel, D. V., Tien, G., Tupas, L., Karl, D. M.: Freezing as a method of
682 sample preservation for the analysis of dissolved inorganic nutrients in seawater, Marine
683 Chemistry, 53(3-4), 173-185, 1996.

684 Fichaut, M., Garcia, M. J., Giorgetti, A., Iona, A., Kuznetsov, A., Rixen, M. and Group, M.:
685 MEDAR/MEDATLAS 2002: A Mediterranean and Black Sea database for operational oceanography,
686 Elsevier Oceanography Series, 69, 645–648, doi:10.1016/S0422-9894(03)80107-1, 2003.

687 Giorgetti, A., Partescano, E., Barth, A., Buga, L., Gatti, J., Giorgi, G., Iona A., Lipizer, M.,
688 Holdsworth, N., Larsen, M.M., Schaap, D., Vinci, M., Wenzer, M. :EMODnet Chemistry Spatial Data
689 Infrastructure for marine observations and related information. *Ocean & Coastal Management*, 166, 9-
690 17, 2018. Giorgi, F.: Climate change hot-spots, *Geophysical Research Letters*, 33(8), 1–4,
691 doi:10.1029/2006GL025734, 2006.

692 Gouretski, V. V. and Jancke, K.: Systematic errors as the cause for an apparent deep water property
693 variability: Global analysis of the WOCE and historical hydrographic data, *Progress in Oceanography*,
694 48(4), 337–402, doi:10.1016/S0079-6611(00)00049-5, 2000.

695 Grasshoff, K., Kremling K., Ehrhardt M.: *Methods of seawater analysis* (3rd ed.), Weinheim
696 Press, WILEY-VCH, 203-273, 1999.

697 Hansen, H. P. and Koroleff, F.: Determination of nutrients, *Methods of Seawater Analysis*, 159–228,
698 1999.

699 Hoppema, M., Velo, A., van Heuven, S., Tanhua, T., Key, R. M., Lin, X., Bakker, D. C. E., Perez, F.
700 F., Ríos, A. F., Lo Monaco, C., Sabine, C. L., Álvarez, M. and Bellerby, R. G. J.: Consistency of
701 cruise data of the CARINA database in the Atlantic sector of the Southern Ocean, *Earth System*
702 *Science Data*, 1(1), 63–75, doi:10.5194/essd-1-63-2009, 2009.

703 Hydes, D. J., Aoyama, M., Aminot, A., Bakker, K., Becker, S., Coverly, S., Daniel, A., Dickson, A. G.,
704 Grosso, O., Kerouel, R., van Ooijen, J., Sato, K., Tanhua, T., Woodward, E. M. S. and Zhang, J. Z.
705 :Determination of Dissolved Nutrients (N, P, SI) in Seawater With High Precision and Inter-
706 Comparability Using Gas-Segmented Continuous Flow Analysers. In: *The GO-SHIP Repeat*
707 *Hydrography Manual: A Collection of Expert Reports and Guidelines. Version 1.* (eds Hood, E.M.,
708 C.L. Sabine, and B.M. Sloyan). IOCCP Report Number 14, ICPO Publication Series Number 134. 87
709 pp., <http://dx.doi.org/10.25607/OBP-555>, 2010.

710

711 Johnson, G. C., Robbins, P. E. and Hufford, G. E.: Systematic adjustments of hydrographic sections
712 for internal consistency, *Journal of Atmospheric Oceanic Technology*, 18(7), 1234–1244,
713 doi:10.1175/1520-0426(2001)018<1234:SAOHSF>2.0.CO;2, 2001.

714 Key, R. M., Kozyr, A., Sabine, C. L., Lee, K., Wanninkhof, R., Bullister, J. L., Feely, R. A., Millero,
715 F. J., Mordy, C. and Peng, T. H.: A global ocean carbon climatology: Results from Global Data
716 Analysis Project (GLODAP), *Global Biogeochem. Cycles*, 18(4), 1–23, doi:10.1029/2004GB002247,
717 2004.

718 Lauvset, S. K. and Tanhua, T.: A toolbox for secondary quality control on ocean chemistry and
719 hydrographic data, *Limnology and Oceanography Methods*, 13(11), 601–608,
720 doi:10.1002/lom3.10050, 2015.

721 Lazzari, P., Solidoro, C., Salon, S. and Bolzon, G.: Spatial variability of phosphate and nitrate in the
722 Mediterranean Sea: A modeling approach, *Deep Sea Research Part I*, 108, 39–52,
723 doi:10.1016/j.dsr.2015.12.006, 2016.

724 Lejeusne, C., Chevaldonné, P., Pergent-Martini, C., Boudouresque, C. F. and Pérez, T.: Climate
725 change effects on a miniature ocean: the highly diverse, highly impacted Mediterranean Sea, *Trends in*

- 726 Ecology and Evolution, 25(4), 250–260, doi:10.1016/j.tree.2009.10.009, 2010.
- 727 Manca, B., Burca, M., Giorgetti, A., Coatanoan, C., Garcia, M. J., and Iona, A. : Physical and
728 biochemical averaged vertical profiles in the Mediterranean regions: an important tool to trace the
729 climatology of water masses and to validate incoming data from operational oceanography. Journal of
730 Marine Systems, 48(1-4), 83-116, 2004.
- 731 Martín Míguez, B., Novellino, A., Vinci, M., Claus, S., Calewaert, J. B., Vallius, H., Schmitt, T.,
732 Pititto, P., Giorgetti, A., Askew, N., Iona, S., Schaap, D., Pinardi, N., Harpham, Q., Kater, B.J.,
733 Populus, J., She, J., Vasilev Palazov, A., McMeel, O., Oset, P., Lear, D., Manzella, G.M.R., Goringe,
734 P., Simoncelli, S., Larkin, K., Holdsworth, N., Dimitrios_Arvanitidis C., Molina-Jack M.E., Chaves-
735 Montero M.D.M. , Herman, P.M.J., and Hernandez F.: The European marine observation and data
736 network (EMODnet): visions and roles of the gateway to marine data in Europe. Frontiers in Marine
737 Science, 6, 2019.
- 738 Moon, J., Lee, K., Tanhua, T., Kress, N. and Kim, I.: Temporal nutrient dynamics in the
739 Mediterranean Sea in response to anthropogenic inputs, , 5243–5251,
740 doi:10.1002/2016GL068788. Received, 2016.
- 741 Muniz, K., Cruzado, A., Ruiz De Villa, C. and Villa, C. R. De: Statistical analysis of nutrient data
742 quality (nitrate and phosphate), applied to useful predictor models in the northwestern Mediterranean
743 Sea, Methodology, 17, 221–231, 2001.
- 744 Olsen, A., Key, R. M., Heuven, S. Van, Lauvset, S. K., Velo, A., Lin, X., Schirnick, C., Kozyr, A.,
745 Tanhua, T., Hoppema, M. and Jutterström, S.: The Global Ocean Data Analysis Project version 2 (
746 GLODAPv2) – an internally consistent data product for the world ocean, , 297–323,
747 doi:10.5194/essd-8-297-2016, 2016.
- 748 Olsen, A., Lange, N., Key, R., Tanhua, T., Alvarez, M. et al.: GLODAPv2.2019 -an update of
749 GLODAPv2. Earth Syst. Sci. Data, 11 (3), pp.1437 - 1461. ff10.5194/essd-11-1437-2019ff. fhal-
750 02315662, 2019.
- 751 Pasqueron, O., Fommervault, D., Migon, C., Ortenzio, F. D., Ribera, M. and Coppola, L.: Temporal
752 variability of nutrient concentrations in the northwestern Mediterranean sea (DYFAMED time-series
753 station), Deep. Res. Part I, 100, 1–12, doi:10.1016/j.dsr.2015.02.006, 2015.
- 754 Powley, H. R., Krom, M. D. and Van Cappellen, P.: Phosphorus and nitrogen trajectories in the
755 Mediterranean Sea (1950–2030): Diagnosing basin-wide anthropogenic nutrient enrichment, Progress
756 in Oceanography, 162, 257–270, doi:10.1016/j.pocean.2018.03.003, 2018.
- 757 Pujo-Pay, M., Conan, P., Oriol, L., Cornet-Barthaux, V., Falco, C., Ghiglione, J. F., Goyet, C.,
758 Moutin, T. and Prieur, L.: Integrated survey of elemental stoichiometry (C, N, P) from the western to
759 eastern Mediterranean Sea, Biogeosciences, 8(4), 883–899, doi:10.5194/bg-8-883-2011, 2011.
- 760 Sabine, C. L., Hoppema, M., Key, R. M., Tilbrook, B., Van Heuven, S., Lo Monaco, C., Metzl, N.,
761 Ishii, M., Murata, A. and Musielewicz, S.: Assessing the internal consistency of the CARINA data
762 base in the Pacific sector of the Southern Ocean, Earth System Science Data Discussions, 2(2), 195–

763 204, doi:10.5194/essd-2-195-2010, 2010.

764 Schroeder, K., Tanhua, T., Bryden, H., Alvarez, M., Chiggiato, J. and Aracri, S.: Mediterranean Sea
765 Ship-based Hydrographic Investigations Program (Med-SHIP), *Oceanography*, 28(3), 12–15,
766 doi:10.5670/oceanog.2015.71, 2015.

767 Schroeder, K., Chiggiato, J., Bryden, H. L., Borghini, M. and Ben Ismail, S.: Abrupt climate shift in
768 the Western Mediterranean Sea, *Scientific Reports*, 1–7, doi:10.1038/srep23009, 2016. Segura-
769 Noguera, M., Cruzado, A. and Blasco, D.: The biogeochemistry of nutrients, dissolved oxygen and
770 chlorophyll a in the Catalan Sea (NW Mediterranean Sea), *Sci. Mar.*, 80(S1), 39–56,
771 doi:10.3989/scimar.04309.20a, 2016.

772 Segura-Noguera, M., Cruzado, A., & Blasco, D.: Nutrient preservation, analysis precision and quality
773 control of an oceanographic database of inorganic nutrients, dissolved oxygen and chlorophyll a from
774 the NW Mediterranean Sea. *Scientia Marina*, 75(2), 321-339, 2011.

775 Suzuki, T., Ishii, M., Aoyama, A., Christian, J. R., Enyo, K., Kawano, T., Key, R. M., Kosugi, N.,
776 Kozyr, A., Miller, L. A., Murata, A., Nakano, T., Ono, T., Saino, T., Sasaki, K., Sasano, D., Takatani,
777 Y., Wakita, M., and Sabine, C. L.: PACIFICA Data Synthesis Project, ORNL/CDIAC-159, NDP-092,
778 Carbon Dioxide Information Analysis Center, Oak Ridge National Laboratory, U. S. Department of
779 Energy, Oak Ridge, Tennessee, 2013.

780 Tanhua, T.: Hydrochemistry of water samples during MedSHIP cruise Talpro. PANGAEA,
781 <https://doi.org/10.1594/PANGAEA.902293>, 2019.

782 Tanhua, T.: Matlab Toolbox to Perform Secondary Quality Control (2nd QC) on Hydrographic Data,
783 ORNL CDIAC-158. Carbon Dioxide Inf. Anal. Center, Oak Ridge Natl. Lab. U.S. Dep. Energy, Oak
784 Ridge, Tennessee, 158, doi:10.3334/CDIAC/otg.CDIAC_158, 2010a.

785 Tanhua, T., Brown, P. J. and Key, R. M.: CARINA : Nutrient data in the Atlantic Ocean, *Earth
786 Science Data*, 1, 7–24, doi:10.3334/CDIAC/otg.CARINA.ATL.V1.0, 2009.

787 Tanhua, T., Heuven, S. van, Key, R. M., Velo, A., Olsen, A. and Schimick, C.: Quality control
788 procedures and methods of the CARINA database, *Earth System Science Data*, 2, 35–49, 2010b.

789 Tanhua, T., Hainbucher, D., Schroeder, K., Cardin, V., Álvarez, M. and Civitarese, G.: The
790 Mediterranean Sea system: A review and an introduction to the special issue, *Ocean Science*, 9(5),
791 789–803, doi:10.5194/os-9-789-2013, 2013.

792 Testor, P., Bosse, A., Houpert, L., Margirier, F., Mortier, L., Legoff, H., Dausse, D., Labaste, M.,
793 Karstensen, J., Hayes, D., Olita, A., Ribotti, A., Schroeder, K., Chiggiato, J., Onken, R., Heslop, E.,
794 Moure, B., D’ortenzio, F., Mayot, N., Lavigne, H., de Fommervault, O., Coppola, L., Prieur, L.,
795 Taillandier, V., Durrieu de Madron, X., Bourrin, F., Many, G., Damien, P., Estoumel, C., Marsaleix,
796 P., Taupier-Letage, I., Raimbault, P., Waldman, R., Bouin, M. N., Giordani, H., Caniaux, G., Somot,
797 S., Ducrocq, V. and Conan, P.: Multiscale Observations of Deep Convection in the Northwestern
798 Mediterranean Sea During Winter 2012–2013 Using Multiple Platforms, *Journal of Geophysical
799 Research: Oceans*, 123(3), 1745–1776, doi:10.1002/2016JC012671, 2018.

800 Tintoré, J., Pinardi, N., Alvarez Fanjul, E., Balbin, R., Bozzano, R., Ferrarin, C.,... and Clementi, E.:
801 Challenges for Sustained Observing and Forecasting Systems in the Mediterranean Sea. *Frontiers in*
802 *Marine Science*, 6, 568, 2019.

803

804 **Figure Captions**

805 **Figure 1.** Map of the Western Mediterranean Sea showing the biogeochemical stations (in blue) and
806 the five reference cruise stations (in red).

807 **Figure 2.** Overview of the reference cruise spatial coverage and vertical distributions of the inorganic
808 nutrients. Top left: geographical distribution map, top right: vertical profiles of nitrate in $\mu\text{mol kg}^{-1}$,
809 bottom left: vertical profiles of phosphate in $\mu\text{mol kg}^{-1}$, bottom right: vertical profiles of silicate in
810 $\mu\text{mol kg}^{-1}$.

811 **Figure 3.** Scatter plots of (A.) phosphate vs nitrate (in $\mu\text{mol kg}^{-1}$) and (B.) silicate vs. nitrate (in μmol
812 kg^{-1}). Data that have been flagged as “questionable” (flag=3) are in red, the colour bar indicates the
813 pressure (in dbar). The black lines represent the best linear fit between the two parameters, and the
814 corresponding equations and r^2 values are shown on each plot. Average resulting N:P ratio is 20.87,
815 average resulting N:Si ratio is 1.05 (whole depth).

816 **Figure 4.** An example of the calculated offset for silicate between cruise 48UR20131015 and cruise
817 29AJ2016818 (reference cruise). Above: location of the stations being part of the crossover and
818 statistics. Bottom left: vertical profiles of silicate data in ($\mu\text{mol kg}^{-1}$) of the two cruises that fall within
819 the minimum distance criteria (the crossing region), below 1000 dbar. Bottom right: vertical plot of
820 the difference between both cruises (dotted black line) with standard deviations (dashed black lines)
821 and the weighted average of the offset (solid red line) with the weighted standard deviations (dotted
822 red line).

823 **Figure 5.** Results of the crossover analysis for nitrate, before (grey) and after adjustment (blue). Error
824 bars indicate the standard deviation of the absolute weighted offset. The dashed lines indicate the
825 accuracy limit 2% for an adjustment to be recommended.

826 **Figure 6.** The same as Fig. 5 but for phosphate.

827 **Figure 7.** The same as Fig. 5 but for silicate.

828 **Figure 8.** Dataset comparison before (black) and after (blue) adjustment, showing vertical profiles of
829 (A.) nitrate (in $\mu\text{mol kg}^{-1}$), (B.) phosphate (in $\mu\text{mol kg}^{-1}$) and (C.) silicate (in $\mu\text{mol kg}^{-1}$). Scatter plots
830 of the adjusted data from all depths after 1st and 2nd quality control for (D.) phosphate vs nitrate (in
831 $\mu\text{mol kg}^{-1}$) and (E.) silicate vs. nitrate (in $\mu\text{mol kg}^{-1}$). The black lines represent the best linear fit
832 between the two parameters, and the corresponding equations and r^2 values are shown on each plot.
833 Average resulting N:P ratio is 22.09, average resulting N:Si ratio is 0.94 (whole depth).

834 **Figure 9.** Vertical profiles of the inorganic nutrients in the dataset after adjustments and spatial
835 coverage of each cruise (reference to cruise ID is above each map). The whole WMED adjusted
836 product is shown in black while the data of each individual cruise are shown in blue (flag=2) and
837 green (flag=3).

838 **Figure 10.** RMSE regional averages of water mass properties computed between the new adjusted
839 product and MEDAR/Medatlas climatology for nitrate (A.), phosphate (B.) and silicate (C.).

840 **Table captions**

841 **Table 1a.** Cruise summary table and parameters listed with number of stations and samples. Cruises
842 were identified with an ID number and expedition code ('EXPOCODE' of format
843 AABBYYYMMDD with AA: country code, BB: ship code, YYYY: year, MM: month, DD: day
844 indicative of cruise starting day).

845 **Table 1b.** Data sources and links to the reports (accessed June 2020).

846 **Table 2.** Cruise summary table of the reference cruises collection used in the secondary quality
847 control, collected from 2001 to 2016.

848 **Table 3.** WOCE flags used in the original data product and in the adjusted product.

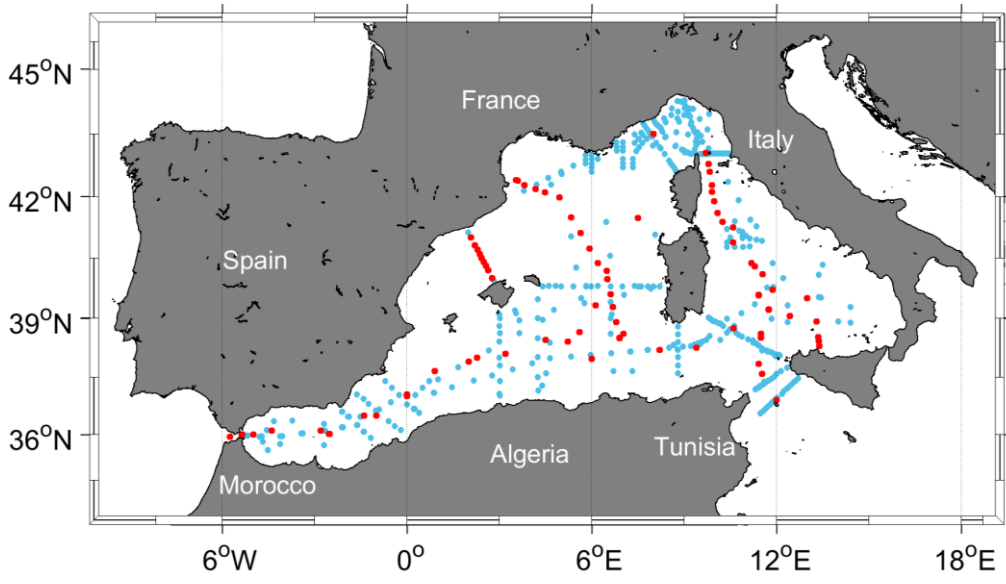
849 **Table 4.** Average and Standard deviations of nitrate, phosphate and silicate measurements by cruise
850 and for each region with number of samples deeper than 1000db included in the 2nd QC. Average
851 storage time: the minimum storage time defined as time difference between the cruise ending day and
852 the 1st day of the laboratory analysis.

853 **Table 5.** Summary of the suggested adjustment for nitrate, phosphate and silicate resulting from the
854 crossover analysis. Adjustments for inorganic nutrient are multiplicative. NA: denotes not adjusted,
855 i.e. data of cruises that could not be used in the crossover analysis, because of the lack of stations or
856 data are outside the spatial coverage of reference cruises.

857 **Table 6.** Secondary QC toolbox results: improvements of the weighted mean of absolute offset per
858 cruise of unadjusted and adjusted data; (n) is the number of crossovers per cruise. The numbers in red
859 (less than 1) indicate that the cruise data are lower than the reference cruises. NA: not adjusted.

860 **Table 7.** Water mass properties and regional average concentrations of inorganic nutrients:
861 comparison between the new adjusted product and the MEDAR/Medatlas climatology (with standard
862 deviations and number of observations in brackets).

863 **Figure 1**



864

865

866

867

868

869

870

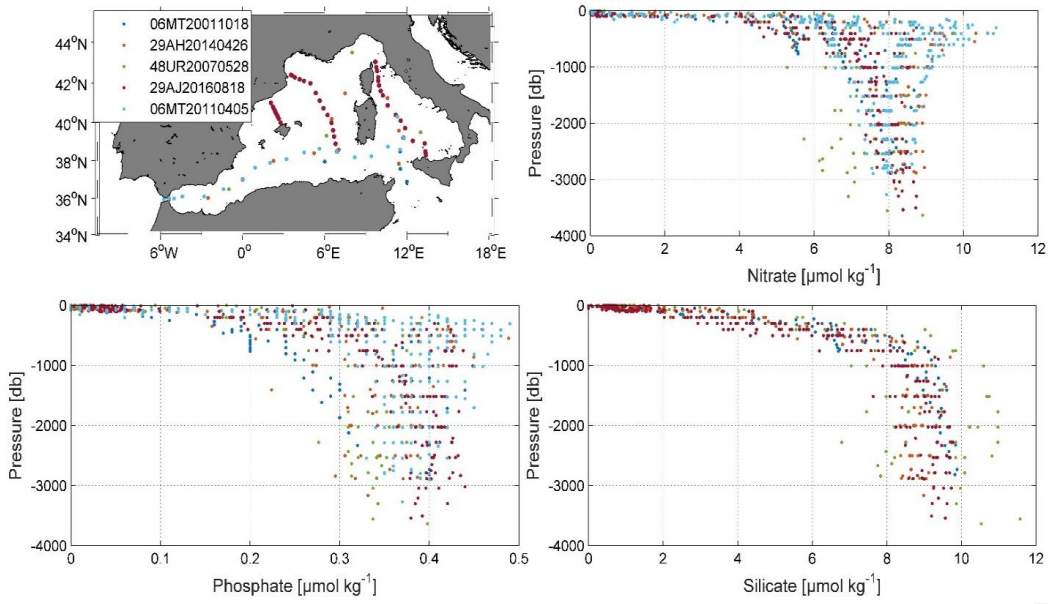
871

872

873

874

875 **Figure 2**



876

877

878

879

880

881

882

883

884

885

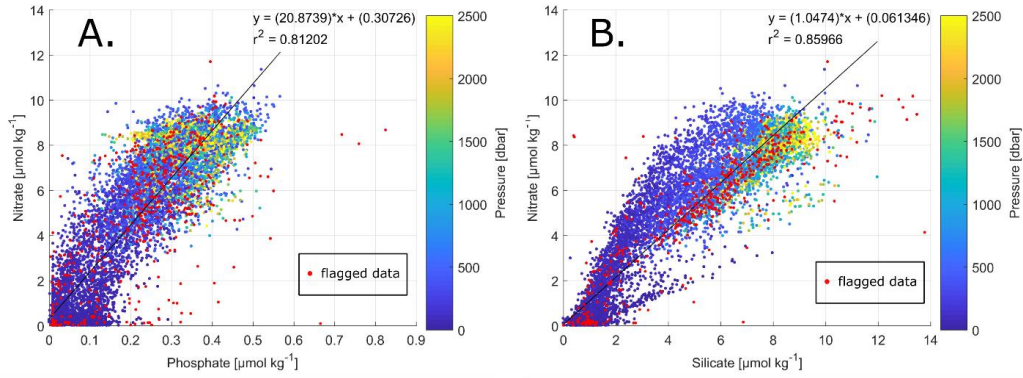
886

887

888

889

890 **Figure 3**



891

892

893

894

895

896

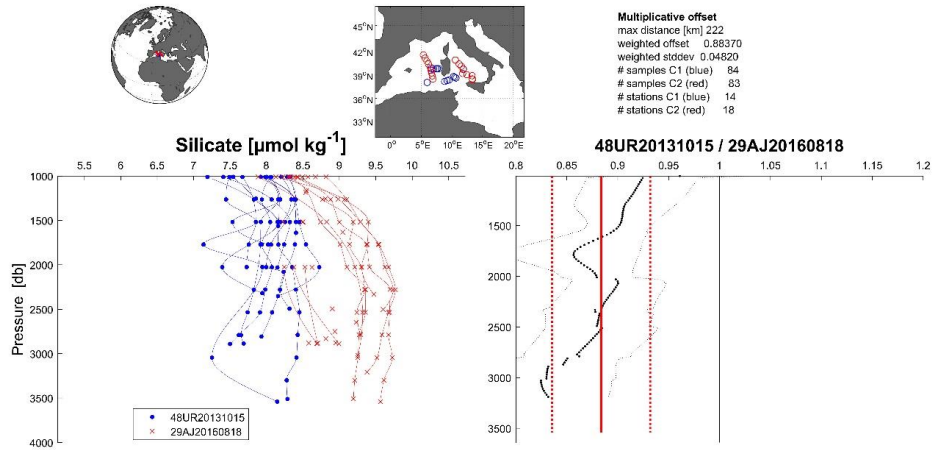
897 **Figure 4**

898

899

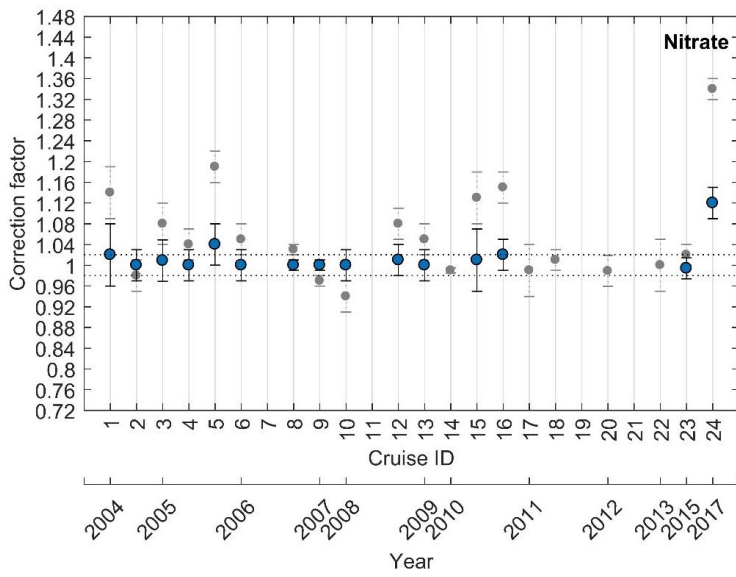
900

901



902

903 **Figure 5**



904

905

906

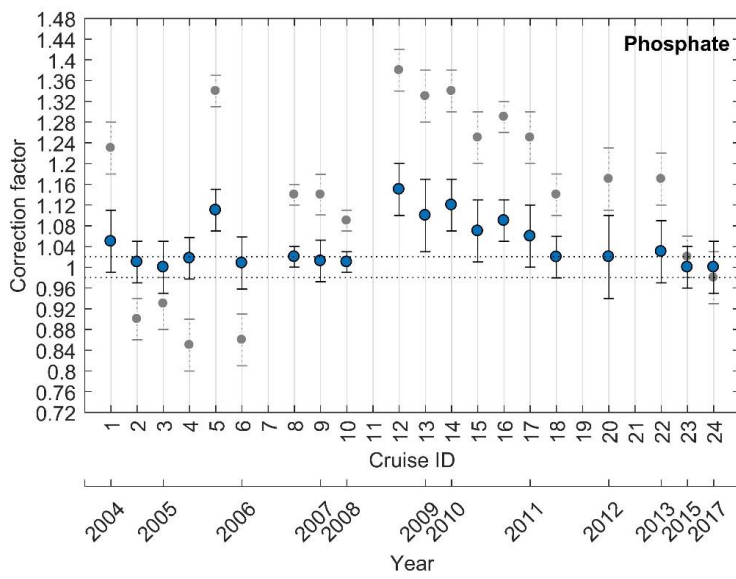
907

908

909

910
911
912
913
914
915
916
917
918
919

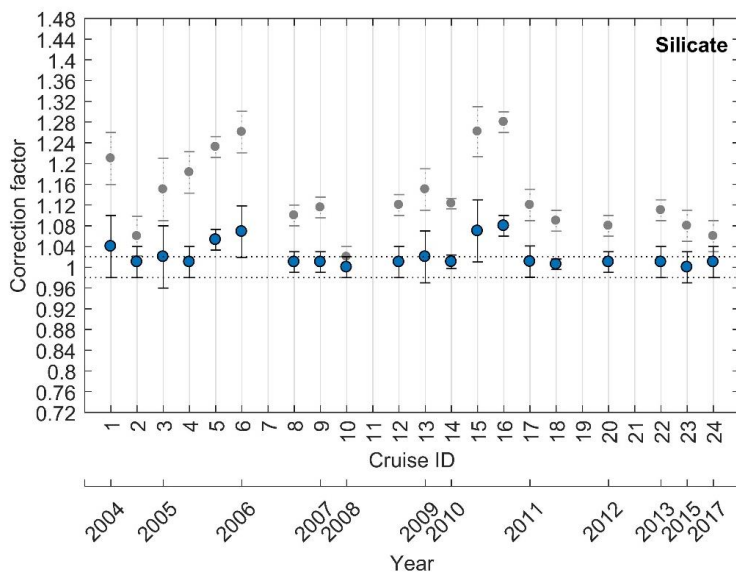
Figure 6



920
921
922
923
924
925

926
927
928
929
930
931
932
933
934
935

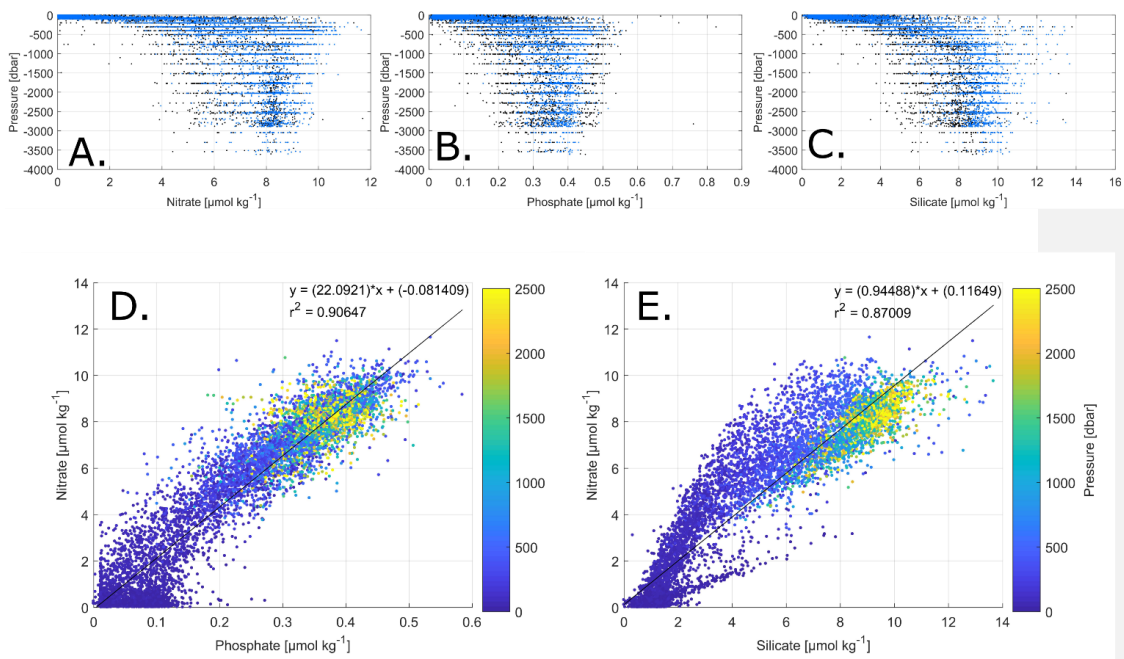
Figure 7



936
937
938
939
940
941

942
943
944
945
946
947
948
949
950
951

Figure 8



952
953
954
955
956

957

958

959

960

961

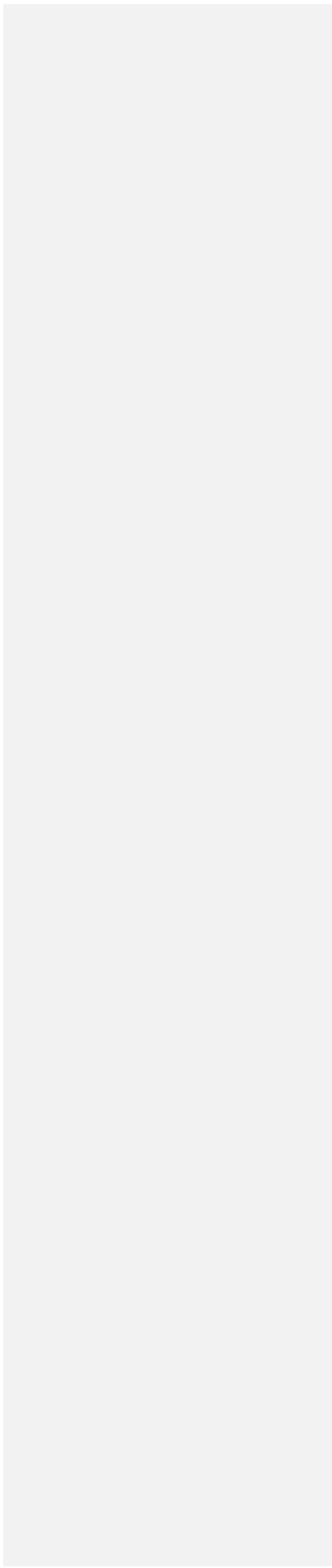
962

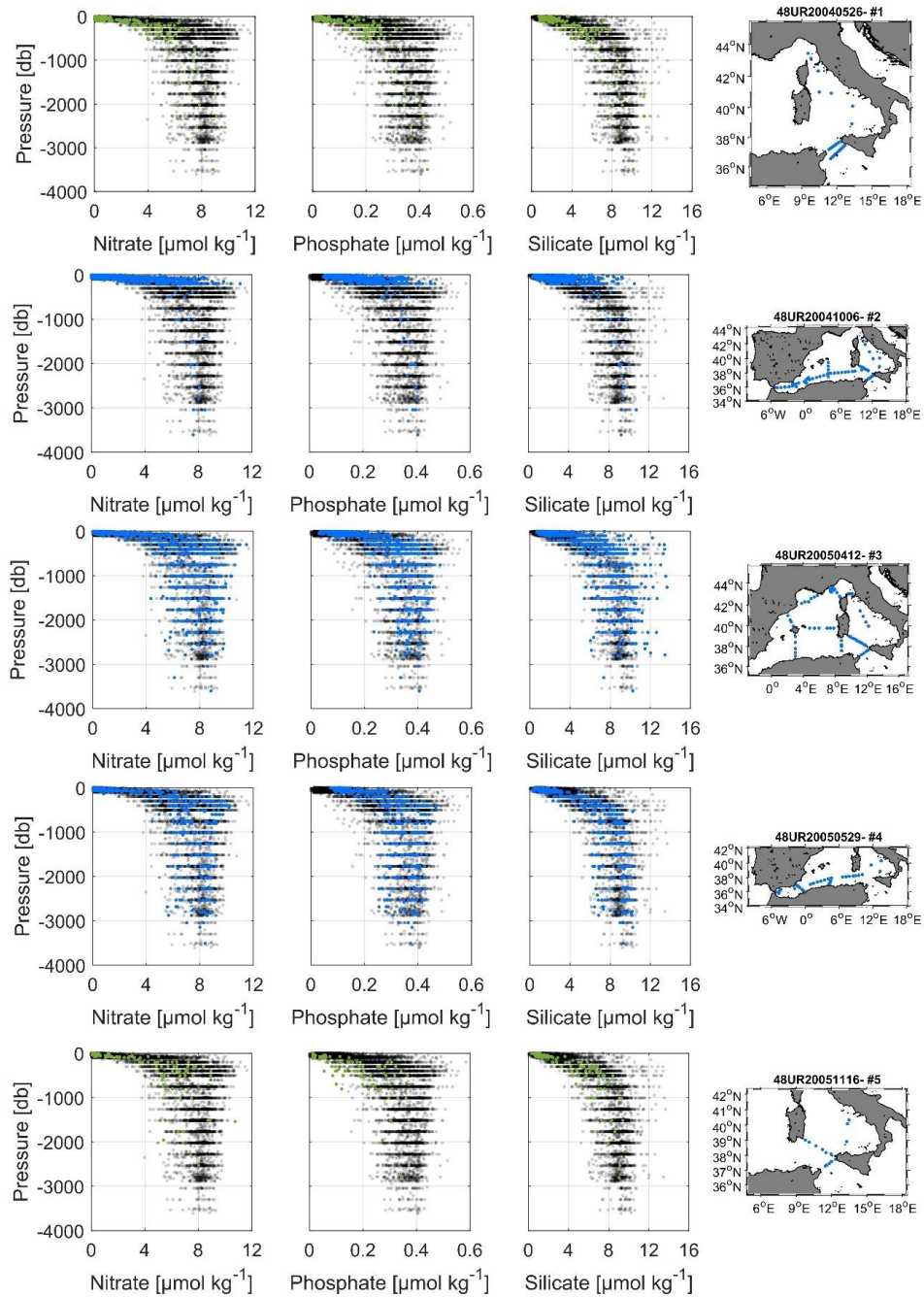
963

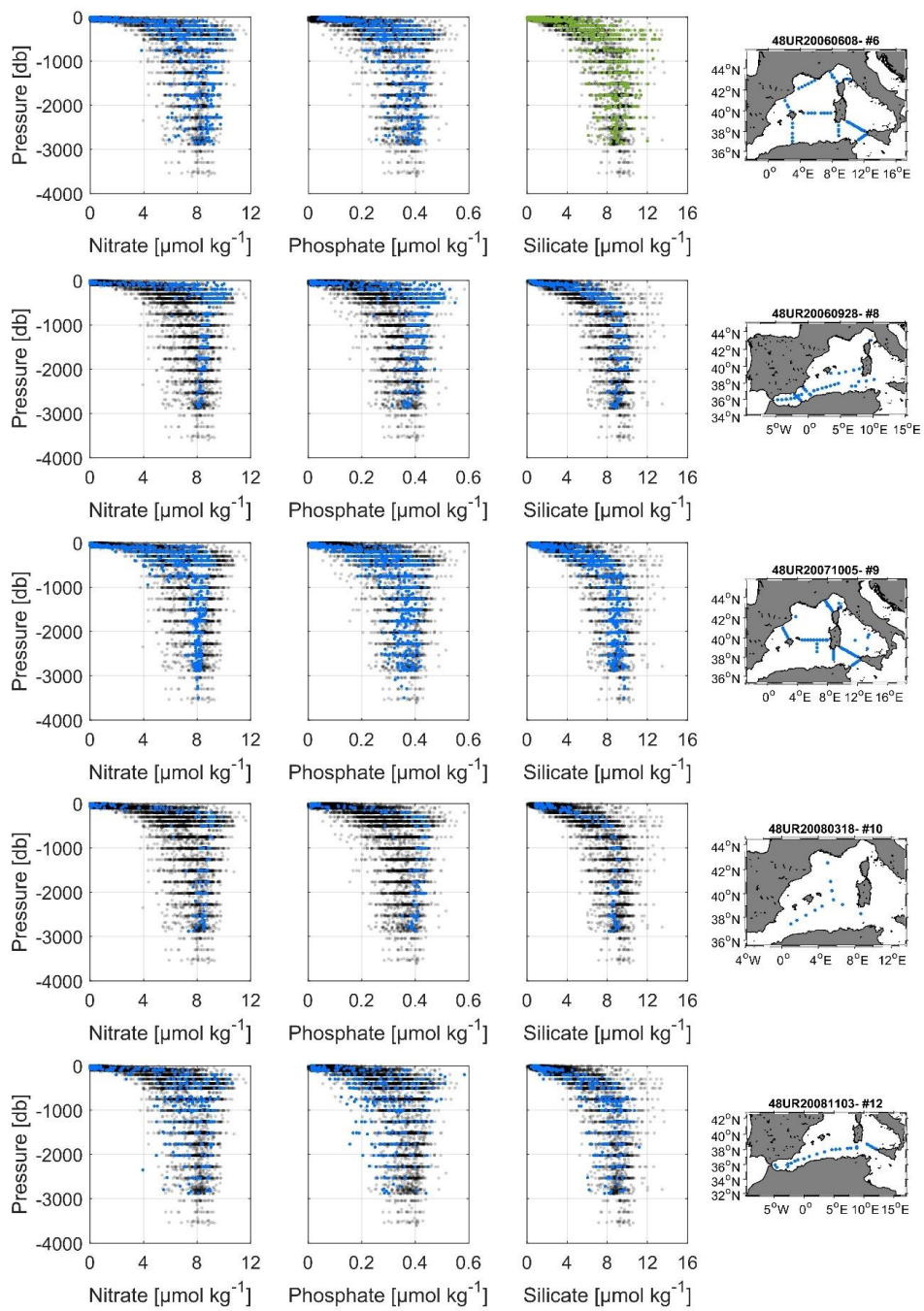
964

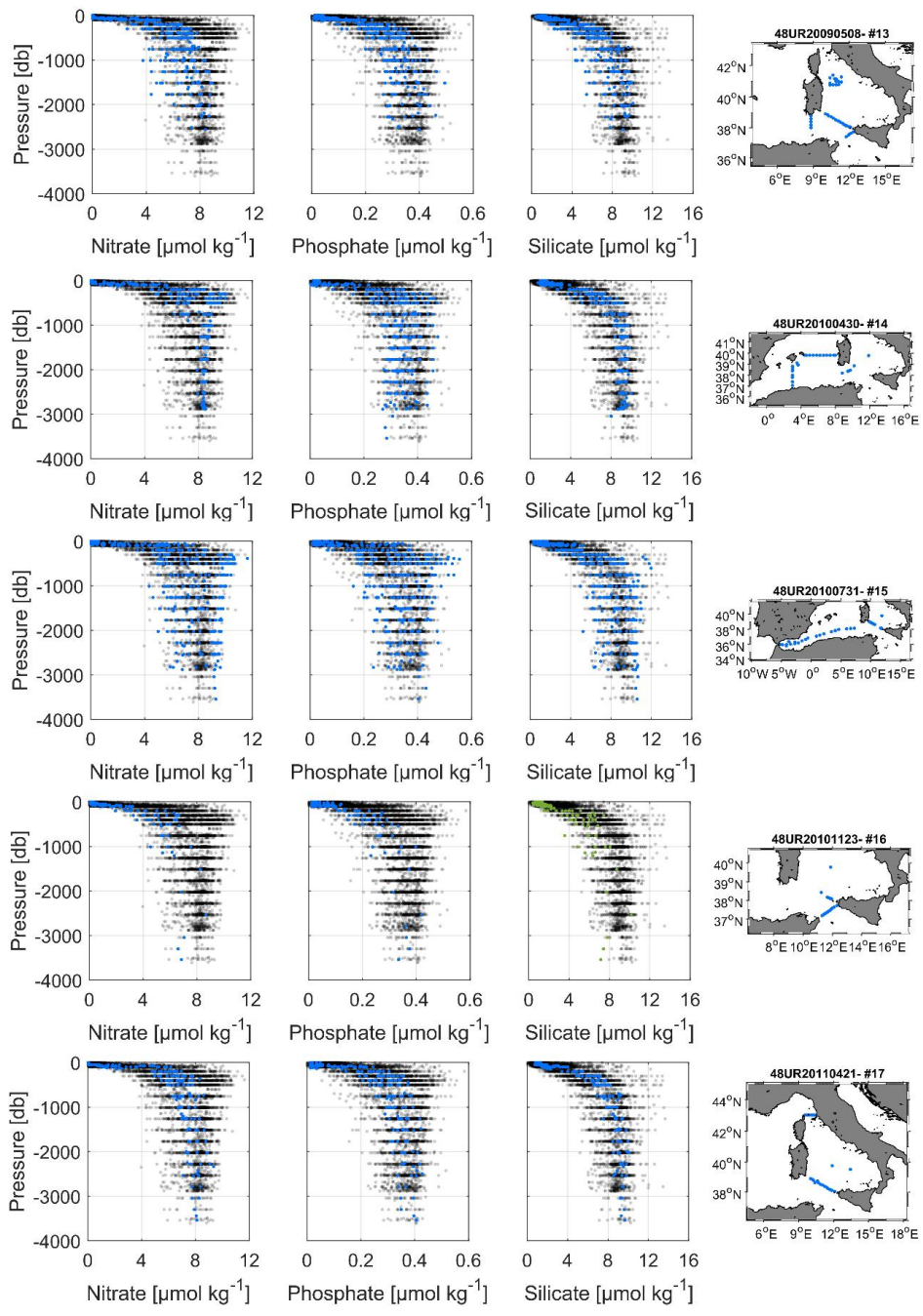
965

966 **Figure 9**



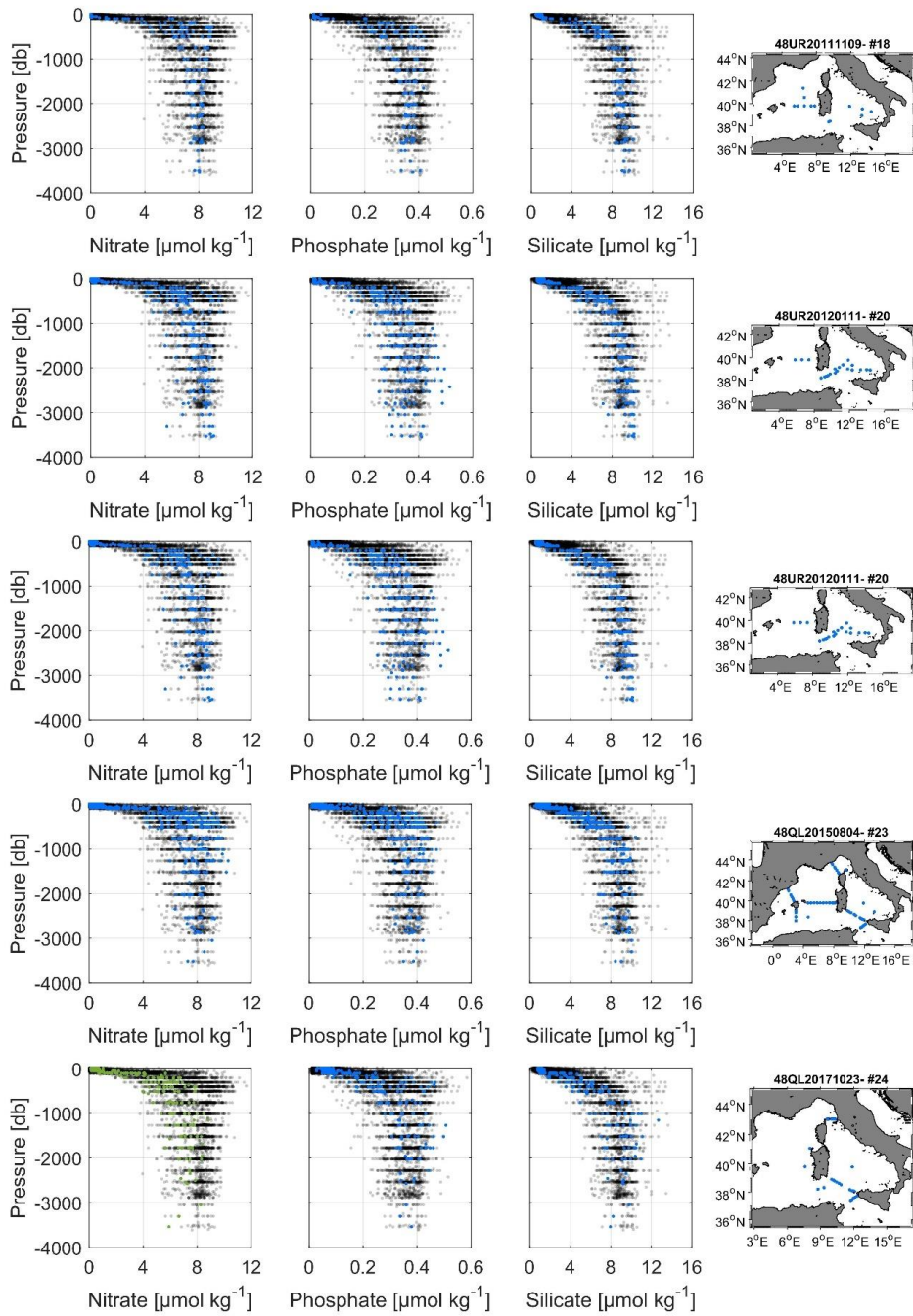






969

970

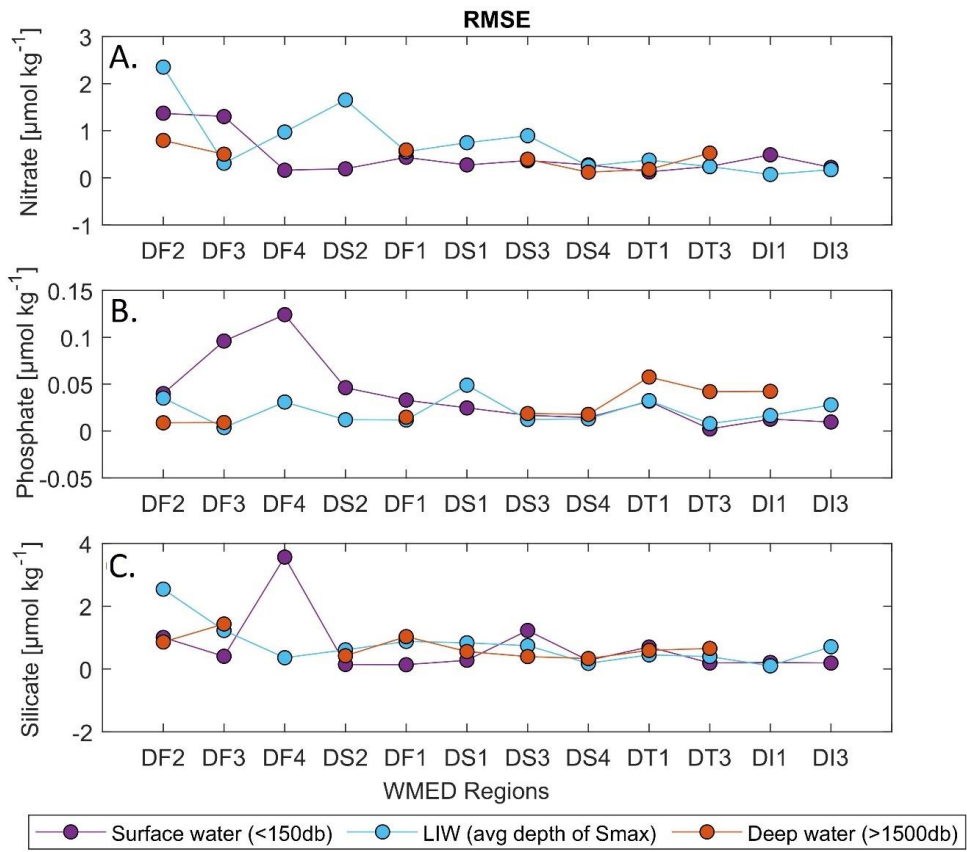


971

972

973 **Figure 10**

974



975

976

977

978

979

980

981

982

983

Table 1a

Cruise ID (#)	Common Name	EXPOCODE	Research vessel (RV)	Date Start/End	Stations	Samples Nitrate	Samples Phosphate	Samples Silicate	Maximum bottom depth (m)	Chief scientist
1	TRENDS2004/MEDGOOS8leg2	48UR20040526	Urania	26 MAY - 14 JUN 2004	36	255	253	255	3499	M. Borghini
2	MEDGOOS9	48UR20041006	Urania	6 - 25 OCT 2004	68	627	626	627	3610	M. Borghini
3	MEDOCC05/MFSTEP2	48UR20050412	Urania	12 APR - 16 MAY 2005	68	828	828	828	3598	M. Borghini
4	MEDGOOS10	48UR20050529	Urania	29 MAY - 10 JUN 2005	36	577	577	577	3505	A. Perilli
5	MEDGOOS11	48UR20051116	Urania	16 NOV - 3 DEC 2005	14	143	143	143	2810	A. Perilli, M. Borghini, M. Dibitto
6	MEDOCC06	48UR20060608	Urania	8 JUN - 3 JUL 2006	66	787	785	787	2881	M. Borghini
7	SIRENA06	06A420060720	NRV Alliance	20 JUL - 6 AUG 2006	35	208	208	209	1854	J. Haun
8	MEDGOOS13/MEDBIO06	48UR20060928	Urania	28 SEP - 8 NOV 2006	37	519	520	520	2862	A. Ribotti
9	MEDOCC07	48UR20071005	Urania	5 - 29 OCT 2007	71	977	977	979	3497	A. Perilli, M. Borghini
10	SESAMEI4	48UR20080318	Urania	18 MAR - 7 APR 2008	11	164	164	164	2882	A. Ribotti
11	SESAMEIT5	48UR20080905	Urania	5 - 16 SEP 2008	12	74	74	74	536	C. Santinelli
12	MEDCO08	48UR20081103	Urania	3 - 24 NOV 2008	24	342	350	348	2880	S. Sparnocchia, G.P. Gasparini, M. Borghini
13	TYRRMOUNTS	48UR20090508	Urania	8 MAY - 3 JUN 2009	41	430	441	440	2559	A. Ribotti
14	BIOFUN010	48UR20100430	Urania	30 APR - 17 MAY 2010	26	405	405	405	3540	G.P. Gasparini
15	VENUS1	48UR20100731	Urania	31 JUL - 25 AUG 2010	32	431	432	428	3544	E. Manini, S. Aliani
16	BONSIC2010	48UR20101123	Urania	23 NOV - 9 DEC 2010	32	431	432	428	3544	G.P. Gasparini, M. Borghini
17	EUROFLEET11	48UR20110421	Urania	21 APR - 8 MAY 2011	18	144	143	143	3540	A. Ribotti
18	BONIFACIO2011	48UR20111109	Urania	9 - 23 NOV 2011	28	277	275	277	3540	G.P. Gasparini, M. Borghini
19	TOSCA2011	48MG20111210	Maria Grazia	10 - 20 DEC 2011	13	180	180	181	3541	A. Ribotti, G. La Spada, M. Borghini
20	ICHNUSSA12	48UR20120111	Urania	11 - 27 JAN 2012	21	310	310	309	2728	M. Borghini
21	EUROFLEET2012	48UR20121108	Urania	8 - 26 NOV 2012	21	353	352	323	3551	A. Ribotti
22	ICHNUSSA13	48UR20131015	Urania	15 - 29 OCT 2013	53	429	434	434	2633	M. Borghini
23	OCEANCERTAIN15	48QL20150804	Minerva Uno	4 - 29 AUG 2015	37	405	404	405	3540	A. Ribotti
24	ICHNUSSA17/INFRAOCE17	48QL20171023	Minerva Uno	23 OCT - 28 NOV 2017	71	531	531	531	3513	J. Chiggiato
					31	251	254	254	3536	A. Ribotti, S. Sparnocchia, M. Borghini

Table 1b

Cruise ID (#)	Expedition original Name	PIs/ Chief scientist	Specific link* (accessed June 2020)
1	TRENDS2004/ MEDGOOS8leg2	M. Borghini	https://isramar.ocean.org.il/perseus_data/CruiseInfo.aspx?criuseid=5821 https://isramar.ocean.org.il/perseus_data/CruiseInfo.aspx?criuseid=4935
2	MEDGOOS9	M. Borghini	Report submission in progress https://isramar.ocean.org.il/perseus_data/CruiseInfo.aspx?criuseid=5823 https://doi.org/10.17882/70340
3	MEDOCC05/ MFSTEP2	M. Borghini	http://ricerca.ismar.cnr.it/CRUISE_REPORTS/2005/URANIA_MEDOCC05.pdf https://isramar.ocean.org.il/perseus_data/CruiseInfo.aspx?criuseid=4936
4	MEDGOOS10	A. Perilli	http://www.seaforecast.cnr.it/it/observation_it.htm https://doi.org/10.17882/70340
5	MEDGOOS11	A. Perilli, M. Borghini, M. Dibitto	http://ricerca.ismar.cnr.it/CRUISE_REPORTS/2005/URANIA_MEDGOOS11_05_REP.pdf https://doi.org/10.17882/70340
6	MEDOCC06	M. Borghini	http://www.seaforecast.cnr.it/reports/Medoc06CR.pdf https://seadata.bsh.de/Cgi-csr/retrieve_sdn2/viewReport.pl?csrref=20106010
7	SIRENA06	J. Haun	Report submission in progress
8	MEDGOOS13/ MEDBIO06	A. Ribotti	http://www.seaforecast.cnr.it/reports/Mebio06-Medg13_CR.pdf https://doi.org/10.17882/70340
9	MEDOCC07	A. Perilli, M. Borghini, A. Ribotti	http://www.seaforecast.cnr.it/reports/Medoc07-MedCo07_Rapp.pdf https://isramar.ocean.org.il/perseus_data/CruiseInfo.aspx?criuseid=5146
10	SESAMEI4	C. Santinelli	https://isramar.ocean.org.il/perseus_data/CruiseInfo.aspx?criuseid=5148 https://emodnet-chemistry.maris.nl/search/details.php?step=0012004~0022017~0153~057104001~058tdin.ntra.phos.slca~00445~0056~00617~00734~0541&count=3592&page=1000&sort=0&header=no
11	SESAMEIT5	S. Sparnocchia, G.P. Gasparini, M. Borghini	https://isramar.ocean.org.il/perseus_data/CruiseInfo.aspx?criuseid=5147
12	MEDCO08	A. Ribotti	http://www.seaforecast.cnr.it/reports/MedCO08_Rapp.pdf
13	TYRRMOUNTS	G.P. Gasparini	Report submission in progress
14	BIOFUN010	E. Manini, S. Aliani	http://www.ismar.cnr.it/products/reports-campagne/2010-2019
15	VENUS1	G.P. Gasparini, M. Borghini	Report submission in progress
16	BONSIC2010	A. Ribotti	http://www.seaforecast.cnr.it/reports/Bonifacio2010Sic_Rapp.pdf
17	EUROFLEET11	G.P. Gasparini, M. Borghini	Report submission in progress
18	BONIFACIO2011	A. Ribotti, G. La Spada, M. Borghini	http://www.seaforecast.cnr.it/reports/Bonifacio2011_Rapp.pdf
19	TOSCA2011	M. Borghini	Report submission in progress
20	ICHNUSSA12	A. Ribotti	http://www.seaforecast.cnr.it/reports/Ichnussa2012_Rapp.pdf
21	EUROFLEET2012	M. Borghini	Report submission in progress
22	ICHNUSSA13	A. Ribotti	http://www.seaforecast.cnr.it/reports/Ichnussa2013_Rapp.pdf
23	OCEANCERTAIN15	J. Chiggiato	https://doi.org/10.1594/PANGAEA.911046 https://doi.pangaea.de/10.1594/PANGAEA.911046
24	ICHNUSSA17/ INFRAOCE17	A. Ribotti, S. Sparnocchia, M. Borghini	Report submission in progress

* The specific links are subjected to updates.

Table 2

Common name	EXPOCODE	Date Start/End	Stations	Nitrate Sample	Phosphate Sample	Silicate Sample	Source	Nutrient PI	Chief scientist
<i>M51/2</i>	06MT20011018	18 OCT - 11 NOV 2001	6	79	79	82	GLODAPv2	B. Schneider	W. Roether
<i>TRANSMED_LEGII</i>	48UR20070528	28 MAY- 12 JUN 2007	4	78	77	78	CARIMED (not yet available)	S. Cozzi, V. Ibbello	M. Azzaro
<i>M84/3</i>	06MT20110405	5 - 28 APR 2011	20	339	343	-	GLODAPv2	G. Civitarese	T. Tanhua
<i>HOTMIX</i>	29AH20140426	26 APR- 31 MAY 2014	18	144	140	144	CARIMED (not yet available)	XA Álvarez-Salgado	J. Aristegui
<i>TALPro-2016</i>	29AJ20160818	18 - 28 AUG 2016	42	293	293	293	MedSHIP programme	L. Coppola	L. Jullion, K. Schroeder

Table 3

WOCE flag value	Interpretation in original dataset	Interpretation in adjusted product
2	Acceptable/ measured	Adjusted and acceptable
3	Questionable/not used	Adjusted and recommended questionable
9	not measured/no data	-

Table 4

Cruise ID	EXPOCODE/ Region	Regional Avg Nitrate (μmol)	std Nitrate	Regional Avg Phosphate	std Phosphate(Regional Avg Silicate (μmol)	std Silicate	# samples	Avg storage (in
-----------	------------------	--	-------------	------------------------	----------------	---	--------------	-----------	-----------------

		kg ⁻¹	($\mu\text{mol kg}^{-1}$)	($\mu\text{mol kg}^{-1}$)	($\mu\text{mol kg}^{-1}$)	kg ⁻¹	($\mu\text{mol kg}^{-1}$)	days
1	48UR20040526/ <i>DT1-Tyrrhenian North</i> <i>DT3-Tyrrhenian South</i>	6.07 7.03	1.25 1.32 0.51	0.26 0.31	0.062 0.065 0.02	6.92 7.66	1.64 1.83 0.53	21 16 5
2	48UR20041006/ <i>DT1-Tyrrhenian North</i> <i>DT3-Tyrrhenian South</i>	7.68 8.17	0.59 0.53 0.60	0.41 0.41	0.029 0.031 0.025	8.74 9.31	0.81 0.75 0.87	21 15 6
3	48UR20050412/ <i>DF2-Gulf of Lion</i> <i>DF3-Liguro-Provençal</i> <i>DS2-Balearic Sea</i> <i>DF1-Algero-Provençal</i> <i>DS3-Algerian West</i> <i>DT1-Tyrrhenian North</i> <i>DT3-Tyrrhenian South</i> <i>DII-Sardinia Channel</i>	7.89 7.45 7.44 7.87 7.7 6.57 6.52 7.22	1.15 0.98 1.08 1.14 1.16 0.816 1.065 1.12 1.065	0.40 0.41 0.40 0.41 0.39 0.36 0.36 0.40	0.050 0.044 0.05 0.039 0.043 0.048 0.047 0.05 0.04	8.17 7.72 7.68 8.88 8.14 7.41 7.56 8.08	1.41 1.065 1.10 1.47 1.96 0.941 1.15 1.42 1.11	233 24 66 21 42 23 21 22 14
4	48UR20050529/ <i>DS1-Alboran Sea</i> <i>DS3-Algerian West</i> <i>DS4-Algerian East</i> <i>DT1-Tyrrhenian North</i> <i>DT3-Tyrrhenian South</i> <i>DII-Sardinia Channel</i>	6.4 7.6 7.48 7.24 7.70 7.58	1.13 1.15 1.13 1.13 0.44 0.38 1.08	0.38 0.41 0.41 0.42 0.41 0.43	0.057 0.041 0.06 0.06 0.03 0.03 0.049	6.26 7.33 7.50 7.91 7.55 7.42	1.08 1.02 0.99 1.23 0.56 0.36 0.82	205 32 73 47 16 14 23
5	48UR20051116/ <i>DT1-Tyrrhenian North</i> <i>DT3-Tyrrhenian South</i> <i>DII-Sardinia Channel</i>	5.68 6.71 6.29	1.35 1.26 1.51 0	0.19 0.20 0.26	0.078 0.08 0.06 0	6.30 6.86 7.53	0.98 0.92 1.065 0	16 10 5 1
6	48UR20060608/ <i>DF2-Gulf of Lion</i> <i>DF3-Liguro-Provençal</i> <i>DS2-Balearic Sea</i> <i>DF1-Algero-Provençal</i> <i>DS3-Algerian West</i> <i>DT3-Tyrrhenian South</i> <i>DII-Sardinia Channel</i>	7.69 8.08 8.06 7.97 8.39 6.39 8.04	1.16 1.02 0.78 0.9 1.16 0.9 1.28 0.85	0.42 0.43 0.43 0.44 0.42 0.36 0.43	0.054 0.04 0.04 0.03 0.03 0.06 0.04	7.089 7.41 7.07 7.34 8.5 6.86 7.77	1.47 1.04 1.21 1.18 1.32 2 1.7 1.25	221 27 35 30 61 28 26 14
7	06A420060720	-	-	-	-	-	-	1367
8	48UR20060928/ <i>DS2-Balearic Sea</i> <i>DF1-Algero-Provençal</i> <i>DS1-Alboran Sea</i> <i>DS3-Algerian West</i> <i>DS4-Algerian East</i> <i>DT3-Tyrrhenian South</i> <i>DII-Sardinia Channel</i>	7.97 8.17 8.2 7.93 7.98 6.2 7.66	0.71 0.17 0.22 0.14 0.89 0.68 1.51 0.6	0.33 0.33 0.35 0.33 0.34 0.28 0.28	0.036 0.017 0.026 0.02 0.03 0.04 0.02	7.84 8.11 8.59 8.09 8.01 6.71 8.00	0.76 0.27 0.3 0.35 0.91 0.7 1.45 0.49	179 4 22 47 70 28 3 5
9	48UR20071005/ <i>DF2-Gulf of Lion</i> <i>DF3-Liguro-Provençal</i> <i>DS2-Balearic Sea</i> <i>DF1-Algero-Provençal</i> <i>DS4-Algerian East</i> <i>DT1-Tyrrhenian North</i> <i>DT3-Tyrrhenian South</i> <i>DII-Sardinia Channel</i>	8.41 8.17 8.17 8.33 8.41 7.83 7.49 7.92	0.89 0.08 1.08 0.43 0.6 0.2 0.41 1.22 1.05	0.31 0.31 0.31 0.32 0.33 0.28 0.28 0.33	0.040 0.01 0.03 0.02 0.018 0.03 0.05 0.02	7.43 7.64 7.58 7.79 7.90 8.26 7.71 8.26	0.86 0.02 1.08 0.39 0.69 0.26 0.55 1.26 0.41	302 4 81 29 82 19 26 38 23
10	48UR20080318/ <i>DF2-Gulf of Lion</i> <i>DS2-Balearic Sea</i> <i>DF1-Algero-Provençal</i> <i>DS3-Algerian West</i> <i>DS4-Algerian East</i> <i>DII-Sardinia Channel</i>	8.54 9.12 9.02 8.93 8.43 7.62	0.51 0.6 0.18 0.36 0.46 0.25 0.6	0.35 0.38 0.38 0.36 0.38 0.34	0.026 0.03 0.01 0.03 0.01 0.02 0.03	8.62 8.40 8.65 8.69 8.32 8.49	0.34 0.43 0.21 0.25 0.35 0.22 0.36	66 5 9 15 20 10 3
11*	48UR20080905	-	-	-	-	-	-	211
12	48UR20081103/ <i>DS1-Alboran Sea</i> <i>DS3-Algerian West</i> <i>DS4-Algerian East</i> <i>DT3-Tyrrhenian South</i> <i>DII-Sardinia Channel</i>	6.4 7.58 7.15 7.44 7.40	1.11 1.21 0.9 1.04 0.5 1.23	0.21 0.27 0.23 0.22 0.17	0.077 0.06 0.1 0.04 0.05 0.04	7.20 7.89 7.38 8.28 8.09	0.10 1.43 0.9 0.9 0.4 0.45	110 26 30 35 10 9
13	48UR20090508/ <i>DT1-Tyrrhenian North</i> <i>DT3-Tyrrhenian South</i> <i>DII-Sardinia Channel</i>	5.95 6.76 7.62	1.41 1.55 0.77 1.1	0.24 0.24 0.28	0.051 0.05 0.03 0.05	6.28 7.37 7.76	1.42 1.58 0.77 0.9	88 46 29 13
14	48UR20100430/ <i>DS2-Balearic Sea</i> <i>DF1-Algero-Provençal</i>	7.66 8.43	1.06 1.6 0.29	0.25 0.26	0.036 0.03 0.03	7.38 8.06	1.03 1.75 0.31	159 33 61

	<i>DS3-Algerian West</i>	8.5	0.14	0.26	0.03	8.25	0.3	26	
	<i>DT1-Tyrrhenian North</i>	6.88	0.8	0.23	0.022	7.17	0.77	11	
	<i>DT3-Tyrrhenian South</i>	6.38	1.35	0.22	0.01	6.76	1.56	7	
	<i>DII-Sardinia Channel</i>	7.71	0.87	0.23	0.02	7.80	0.74	21	
15	48UR20100731/		1.34		0.053		0.14	149	213
	<i>DS1-Alboran Sea</i>	7.30	1.18	0.29	0.05	7.21	1.11	25	
	<i>DS3-Algerian West</i>	7.67	1.15	0.28	0.045	7.24	1.16	54	
	<i>DS4-Algerian East</i>	7.38	0.89	0.29	0.03	7.00	0.78	29	
	<i>DT1-Tyrrhenian North</i>	7.66	0.96	0.29	0.05	7.89	1.07	10	
	<i>DT3-Tyrrhenian South</i>	5.4	0.67	0.22	0.01	5.52	1.56	30	
	<i>DII-Sardinia Channel</i>	4.92	0	0.20	0	5.55	0	1	
16	48UR20101123/		1.02		0.045		1.02	14	170
	<i>DT1-Tyrrhenian North</i>	6.34	0.87	0.27	0.02	6.12	0.87	8	
	<i>DT3-Tyrrhenian South</i>	5.43	1.02	0.22	0.04	5.08	0.9	6	
17	48UR20110421/		0.62		0.029		0.52	56	160
	<i>DT1-Tyrrhenian North</i>	7.77	0.45	0.28	0.02	8.11	0.35	21	
	<i>DT3-Tyrrhenian South</i>	7.76	0.7	0.28	0.03	8.017	0.6	35	
18	48UR20111109/		0.68		0.025		0.70	77	74
	<i>DF3-Liguro-Provençal</i>	6.68	0	0.33	0	6.26	0	1	
	<i>DF1-Algero-Provençal</i>	8.17	0.5	0.32	0.01	8.16	0.66	43	
	<i>DT1-Tyrrhenian North</i>	7.26	0.93	0.29	0.02	8.15	1.03	12	
	<i>DT3-Tyrrhenian South</i>	7.61	0.37	0.30	0.02	8.18	0.35	11	
	<i>DII-Sardinia Channel</i>	7.64	0.45	0.29	0.01	8.08	0.41	10	
19*	48MG20111210		-		-		-	-	38
20	48UR20120111/		0.97		0.051		0.26	152	317
	<i>DF1-Algero-Provençal</i>	8.45	0.49	0.31	0.039	7.91	0.53	23	
	<i>DT1-Tyrrhenian North</i>	7.67	0.83	0.27	0.02	8.29	0.8	30	
	<i>DT3-Tyrrhenian South</i>	7.65	1.06	0.31	0.06	8.03	1.26	69	
	<i>DII-Sardinia Channel</i>	7.65	0.96	0.31	0.03	7.86	0.78	30	
21*	48UR20121108		-		-		-	-	72
22	48UR20131015/		1.03		0.043		0.79	98	76
	<i>DF1-Algero-Provençal</i>	8.54	0.64	0.33	0.02	7.96	0.38	36	
	<i>DS4-Algerian East</i>	7.67	1.28	0.27	0.04	6.82	1.07	8	
	<i>DT1-Tyrrhenian North</i>	6.47	0.83	0.24	0.025	7.12	0.84	10	
	<i>DT3-Tyrrhenian South</i>	7.81	0.71	0.30	0.03	8.09	0.65	28	
	<i>DII-Sardinia Channel</i>	7.32	0.99	0.27	0.02	7.47	0.89	16	
23	48QL20150804/		0.84		0.038		0.85	94	30
	<i>DF3-Liguro-Provençal</i>	8.51	0.96	0.39	0.03	8.06	0.85	23	
	<i>DS2-Balearic Sea</i>	7.75	0.66	0.36	0.02	7.86	0.81	20	
	<i>DF1-Algero-Provençal</i>	7.9	0.59	0.37	0.03	8.34	0.68	23	
	<i>DS3-Algerian West</i>	7.84	0.67	0.36	0.02	7.75	0.68	6	
	<i>DT1-Tyrrhenian North</i>	7.92	0.61	0.37	0.02	8.75	0.4	8	
	<i>DT3-Tyrrhenian South</i>	7.23	0.75	0.34	0.025	8.2	0.94	13	
	<i>DII-Sardinia Channel</i>	6.30	0	0.25	0	5.36	0	1	
24	48QL20171023/		0.68		0.055		1.24	55	30
	<i>DF3-Liguro-Provençal</i>	6.63	0.41	0.40	0.05	10.76	1.07	3	
	<i>DF1-Algero-Provençal</i>	5.14	0.7	0.43	0.02	7.94	1.19	6	
	<i>DT1-Tyrrhenian North</i>	4.98	0.58	0.36	0.02	8.10	0.87	9	
	<i>DT3-Tyrrhenian South</i>	5.43	0.5	0.36	0.04	9.03	0.87	26	
	<i>DII-Sardinia Channel</i>	5.16	0.76	0.41	0.07	7.58	1.17	11	

(*): cruise not included in the 2ndQC (Section 4.)

in bold: the overall standard deviation by cruise; in normal font: regional standard deviation by cruise

Table 5

Cruise ID	EXPOCODE	Nitrate (x)	Phosphate (x)	Silicate (x)
1	48UR20040526	1.14	1.23	1.21
2	48UR20041006	0.98	0.9	1.06
3	48UR20050412	1.08	0.93	1.15
4	48UR20050529	1.04	0.85	1.183
5	48UR20051116	1.19	1.34	1.232

6	48UR20060608	1.05	0.86	1.261
7	06A420060720*	-	-	-
8	48UR20060928	1.03	1.14	1.1
9	48UR20071005	0.97	1.14	1.115
10	48UR20080318	0.94	1.09	1.02
11	48UR20080905*	-	-	-
12	48UR20081103	1.08	1.38	1.12
13	48UR20090508	1.05	1.33	1.15
14	48UR20100430	NA	1.34	1.123
15	48UR20100731	1.13	1.25	1.262
16	48UR20101123	1.15	1.29	1.28
17	48UR20110421	NA	1.25	1.12
18	48UR20111109	NA	1.14	1.09
19	48MG20111210*	-	-	-
20	48UR20120111	NA	1.17	1.08
21	48UR20121108*	-	-	-
22	48UR20131015	NA	1.17	1.11
23	48QL20150804	1.02	1.02	1.08
24	48QL20171023	1.34	0.98	1.06

(*) cruise not included in the 2ndQC (Section 4.)

Table 6

Cruise ID	EXPOCODE	Nitrate [%]			Phosphate[%]			Silicate[%]		
		<i>n</i>	<i>unadjusted</i>	<i>adjusted</i>	<i>n</i>	<i>unadjusted</i>	<i>adjusted</i>	<i>n</i>	<i>unadjusted</i>	<i>adjusted</i>
1	48UR20040526	2	0.86	0.98	2	0.77	0.95	1	0.79	0.96
2	48UR20041006	2	1.02	1.00	2	1.10	0.99	1	0.94	0.99
3	48UR20050412	5	0.92	0.99	5	1.07	1.00	4	0.85	0.98
4	48UR20050529	5	0.96	1.00	5	1.15	0.98	4	0.82	0.99
5	48UR20051116	2	0.81	0.96	1	0.66	0.89	1	0.77	0.95
6	48UR20060608	5	0.95	1.00	5	1.14	0.99	4	0.74	0.93
7	06A420060720	0	-	-	0	-	-	0	-	-
8	48UR20060928	4	0.97	1.00	4	0.86	0.98	3	0.90	0.99
9	48UR20071005	5	1.03	1.00	5	0.86	0.98	4	0.88	0.99
10	48UR20080318	3	1.06	1.00	3	0.91	0.99	2	0.98	1.00
11	48UR20080905	0	-	-	0	-	-	0	-	-
12	48UR20081103	5	0.92	0.99	5	0.62	0.85	4	0.88	0.99
13	48UR20090508	3	0.95	1.00	3	0.67	0.90	2	0.85	0.98
14	48UR20100430	4	1.01	NA	4	0.66	0.88	3	0.88	0.99
15	48UR20100731	5	0.87	0.99	5	0.75	0.93	4	0.74	0.93
16	48UR20101123	1	0.85	0.98	1	0.71	0.91	1	0.72	0.92
17	48UR20110421	2	1.01	NA	2	0.75	0.94	1	0.88	0.99
18	48UR20111109	4	0.99	NA	4	0.86	0.98	3	0.91	0.99
19	48MG20111210	0	-	-	0	-	-	0	-	-
20	48UR20120111	4	1.01	NA	4	0.83	0.98	3	0.92	0.99
21	48UR20121108	0	-	-	0	-	-	0	-	-
22	48UR20131015	4	1.00	NA	4	0.83	0.97	3	0.89	0.99
23	48QL20150804	5	0.98	1.00	5	0.98	1.00	4	0.92	1.00
24	48QL20171023	3	0.66	0.88	3	1.02	1.00	2	0.94	0.99

red: data lower than reference

Table 7

Region/ Water mass	Nitrate ($\mu\text{mol kg}^{-1}$)		Phosphate ($\mu\text{mol kg}^{-1}$)		Silicate ($\mu\text{mol kg}^{-1}$)	
	Avg new Product	Avg Medar	Avg new Product	Avg Medar	Avg new Product	Avg Medar
<i>DF2- Gulf of Lion</i>						
surface water (0-150db)	2.68±2.53(68)**	1.7±1.1	0.15±0.06(68)	0.13±0.04	2.91±1.33(68)	1.72±0.64
LIW core (S_{max} depth range: 300-500db)	8.49±0.18(17)	6.13±0.32	0.38±0.02(17)	0.34±0.01	8.67±0.69(17)	6.12±0.61
Deep water (>1500db)	8.03±0.43(33)	7.64±0.31	0.37±0.01(33)	0.37±0.015	8.7±0.67(33)	7.95±0.06
<i>DF3- Liguro-Provençal</i>						
surface water (0-150db)	2.31±2.4(205)	3.0±2.6	0.12±0.07(205)	0.19±0.05	2.45±1.05(205)	2.16±1.05
LIW core (S_{max} depth range: 300-500db)	8.05±0.18(76)	7.74±0.13	0.36±0.01(76)	0.35±0.01	7.49±0.55(76)	6.26±0.60
Deep water (>1500db)	8.18±0.25(142)	7.79±0.04	0.37±0.02(142)	1.03±1.29	8.98±0.39(142)	7.60±0.21
<i>DF4- Ligurian East</i>						
surface water (0-150db)	0.7±0.69(228)	0.61±1.03	0.05±0.02(228)	0.18±0.02	1.37±0.45(228)	1.27±1.86
LIW core (S_{max} depth range: 300-500db)	6.8±0.4(23)	5.54±0	0.3±0.02(21)	0.36±0.06	5.86±0.9(24)	4.86±0
Deep water (>1500db)	-	-	-	-	-	-
<i>DS2- Balearic Sea</i>						
surface water (0-150db)	1.32±1.46(196)	1.19±1.5	0.08±0.04(196)	0.11±0.04	1.61±0.64(196)	1.54±0.78
LIW core (S_{max} depth range: 300-500db)	8.32±0.32(58)	6.92±0.12	0.37±0.02(60)	0.39±0.003	7.31±0.9(60)	7.55±0.62
Deep water (>1500db)	8.2±0.35(88)	-	0.37±0.01(88)	-	8.71±0.51(88)	8.45±0.8
<i>DF1- Algero-Provençal</i>						
surface water (0-150db)	0.87±0.85(372)	1.08±1.7	0.05±0.02(372)	0.07±0.05	1.42±0.3(372)	1.28±0.73
LIW core (S_{max} depth range: 300-500db)	8.07±0.34(126)	7.51±0.18	0.36±0.02(126)	0.34±0.008	6.84±0.95(126)	5.96±0.77
Deep water (>1500db)	8.36±0.27(300)	7.87±0.13	0.38±0.02(300)	0.38±0.001	9.01±0.33(300)	8.18±0.10
<i>DS1- Alboran Sea</i>						
surface water (0-150db)	2.75±2.87(299)	2.51±2.23	0.17±0.11(299)	0.16±0.07	2.07±1.38(299)	2.31±1.14
LIW core (S_{max} depth range: 400-600db)	8.89±0.4(77)	8.14±0.11	0.42±0.02(77)	0.37±0.008	8.77±1.66(76)	7.95±0.34
Deep water (>1500db)	7.72±0.81(65)	-	0.36±0.04(65)	-	8.98±0.63(65)	8.16±0
<i>DS3- Algerian West</i>						
surface water (0-150db)	1.8±1.88(254)	1.82±2.01	0.11±0.05(354)	0.11±0.06	1.71±0.68(354)	2.10±0.91
LIW core (S_{max} depth range: 400-600db)	9.33±0.08(70)	8.28±0.15	0.41±0(73)	0.38±0.012	8.1±0.53(72)	6.68±0.80
Deep water (>1500db)	8.37±0.27(246)	8.047±0.013	0.37±0.02(246)	0.36±0.006	9.22±0.35(246)	8.87±0.23
<i>DS4- Algerian East</i>						
surface water (0-150db)	0.94±0.77(170)	0.75±1.26	0.07±0.02(170)	0.05±0.03	1.53±0.12(170)	1.35±0.52
LIW core (S_{max} depth range: 400-600db)	8.5±0.25(43)	8.60±0.06	0.38±0.03(43)	0.38±0.008	7.27±0.67(42)	7.092±0.55
Deep water (>1500db)	7.94±0.24(132)	8.06±0.06	0.36±0.02(132)	0.38±0.006	8.73±0.38(132)	9.04±0.24
<i>DT1- Tyrrhenian North</i>						
surface water (0-150db)	1.03±1.14(231)	0.88±1.2	0.06±0.02(231)	0.09±0.03	1.64±0.52(231)	2.19±0.59
LIW core (S_{max} depth range: 400-600db)	5.95±0.49(43)	5.86±0.36	0.27±0.03(44)	0.308±0.02	7.06±0.08(44)	6.76±0.59
Deep water (>1500db)	7.75±0.37(194)	7.12±0.47	0.36±0.03(194)	0.40±0.02	9.19±0.47(194)	7.51±0.49
<i>DT3- Tyrrhenian South</i>						
surface water (0-150db)	1.21±1.38(711)	1.23±1.80	0.06±0.03(711)	0.061±0.04	1.58±0.61(711)	1.55±1.05
LIW core (S_{max} depth range: 300-500db)	6.2±0.28(225)	6.42±0.01	0.26±0.02(225)	0.254±0.005	6.28±0.65(224)	6.68±0.44
Deep water (>1500db)	7.88±0.4(227)	7.12±0.26	0.37±0.02(227)	0.31±0.007	9.04±0.52(227)	8.02±0.07
<i>DII- Sardinia Channel</i>						
surface water (0-150db)	1.22±1.39(271)	1.42±1.95	0.07±0.03(271)	0.064±0.03	1.57±0.68(271)	1.39±1.01
LIW core (S_{max} depth range: 300-500db)	6.52±0.17(89)	6.45±0.22	0.27±0.02(89)	0.250±0.01	6.36±0.67(89)	6.27±0.70
Deep water (>1500db)	7.91±0.62(107)	-	0.37±0.03(107)	0.32±0	8.64±0.91(107)	-
<i>DI3- Sicily Strait</i>						
surface water (0-150db)	0.87±0.68(583)	0.77±0.81	0.06±0.02(583)	0.063±0.02	1.53±0.29(583)	1.44±0.58
LIW core (S_{max} depth range: 200-400db)	4.95±0.47(80)	5.14±0.14	0.21±0.02(78)	0.194±0.004	5.26±0.79(81)	6.744±0.41
Deep water (>1500db)	-	-	-	-	-	-

**Average (Avg) ± standard deviation of inorganic nutrient (the number observation within depth range) for three layers from the adjusted/new product and MEDATLAS vertical climatological profiles (called here Medar). Regions are defined according to Manca et al. (2004) (table 2S, Fig.2S)